Published in final edited form as:
Neuroscience. 2006 December 1; 143(2): 547–564.

Subcellular Localization of NADPH Oxidase Subunits in Neurons and Astroglia of the Rat medial Nucleus Tractus Solitarius: Relationship with Tyrosine Hydroxylase Immunoreactive Neurons

Michael J. Glass, **Jie Huang**, **Martin Oselkin**, **M. Jacqueline Tarsitano**, **Gang Wang**, **Costantino Iadecola**, and **Virginia M. Pickel**
Department of Neurology and Neuroscience, Weill Medical College of Cornell University, New York, NY 10021, USA

Abstract

Superoxide produced by the enzyme NADPH oxidase mediates crucial intracellular signaling cascades in the mNTS, a brain region populated by catecholaminergic neurons, as well as astroglia that play an important role in autonomic function. The mechanisms mediating NADPH oxidase (phox) activity in the neural regulation of cardiovascular processes are incompletely understood, however the subcellular localization of superoxide produced by the enzyme is likely to be an important regulatory factor. We used immunogold electron microscopy to determine the phenotypic and subcellular localization of the NADPH oxidase subunits $p47^{phox}$, $gp91^{phox,}$ and $p22^{phox}$ in the mNTS. The mNTS contains a large population of neurons that synthesize catecholamines. Significantly, catecholaminergic signaling can be modulated by redox reactions. Therefore, the relationship of NADPH oxidase subunit labeled neurons or glia with respect to catecholaminergic neurons was also determined by dual labeling for the superoxide producing enzyme and tyrosine hydroxylase (TH), the rate-limiting enzyme in catecholamine biosynthesis. In the mNTS, NADPH oxidase subunits were present primarily in somatodendritic processes and astrocytes, some of which also contained TH, or were contacted by TH labeled axons, respectively. Immunogold quantification of NADPH oxidase subunit localization showed that $p47^{phox}$ and $gp91^{phox}$ were present on the surface membrane, as well as vesicular organelles characteristic of calcium storing smooth endoplasmic reticula in dendritic and astroglial processes. These results indicate that NADPH oxidase assembly and consequent superoxide formation are likely to occur near the plasmalemma, as well as on vesicular organelles associated with intracellular calcium storage within mNTS neurons and glia. Thus, NADPH oxidase-derived superoxide may participate in intracellular signaling pathways linked to calcium regulation in diverse mNTS cell types. Moreover, NADPH oxidase-derived superoxide in neurons and glia may directly or indirectly modulate catecholaminergic neuron activity in the mNTS.

Keywords

autonomic nervous system; blood pressure; catecholamines; reactive oxygen species; superoxide

Corresponding Author: Michael J. Glass, Ph.D, Department of Neurology and Neuroscience, Weill Medical College of Cornell University, 411 E. 69th St., KB410, New York, NY 10021.

Introduction

A critical central coordinator of cardiorespiratory processes, the nucleus of the solitary tract (NTS) is known to modulate systemic arterial pressure (Aicher et al., 2000), cerebral blood flow (Agassandian et al., 2003), respiration (Gozal et al., 2000), and energy balance (Glass et al., 2002). This global modulation is directly related to its unique synaptic organization, which includes the first central synapse of glutamatergic mechano- and chemoreceptor, as well as afferents from the circumventricular organ the area postrema, and other areas of the brainstem-forebrain autonomic neuraxis, including the rostral ventrolateral medulla and amygdala (Barraco, 1994).

Within the mNTS, a wide array of signaling molecules, including small amino acid transmitters, as well as catecholamine and peptide modulators, have been implicated in coordinating autonomic, and particularly cardiovascular processes (Lawrence and Jarrott, 1996). Angiotensin II (ANGII)-induced activation of angiotensin AT-1A receptors in the mNTS has been shown to be an important inhibitor of the baroreflex (Diz et al., 2001), an effect that may be mediated by production of reactive oxygen species (ROS). Indeed, in addition to mediating hypertension-induced cellular plasticity in the peripheral vasculature (Zimmerman and Davisson, 2004, Chan et al., 2005), reactive oxygen is also an important molecular substrate of central autonomic regulation (Zimmerman and Davisson, 2004). For example, the production of ROS within central autonomic pathways is associated with sympathetic nervous system activation (Campese et al., 2004), including stress-induced autonomic activation (Mayorov et al., 2004), as well as salt-induced stroke in stroke-prone spontaneously hypertensive rats (Kim-Mitsuyama et al., 2005).

Many detrimental effects of neurogenic hypertension are mediated by superoxide generated via NADPH oxidase (Wang et al., 2004, Zimmerman and Davisson, 2004, Zimmerman et al., 2005). This enzyme was first described in phagocytes (Lassègue and Clempus, 2003), but is now known to be present in diverse cell types (Serrano et al., 2003, Tejada-Simon et al., 2005, Vallet et al., 2005), including NTS neurons (Wang et al., 2004). NADPH oxidase is comprised of two membrane-bound subunits, $gp91^{phox}$ and $p22^{phox}$, several mobile cytoplasmic subunits including, $p40^{phox}$, and $p67^{phox}$, and the essential $p47^{phox}$, as well as the small GTPase RAC (Lambeth, 2004, Sumimoto et al., 2005). NADPH oxidase activation can be triggered by intracellular calcium, such as that induced by stimulation of the AT-1A receptor subtype, with subsequent phosphorylation and membrane translocation of $p47^{phox}$ to the $gp91^{phox}$ subunit (Cai et al., 2003, Taniyama and Griendling, 2003).

The subcellular location of superoxide generation is an important factor in redox modulation of intracellular signaling pathways (Wolin, 2004). Significantly, the subcellular location of NADPH oxidase subunits is dependent on cell phenotype. For example, phagocyte $p47^{phox}$ is located within the cytosol, and upon phosphorylation it couples with the predominantly plasmalemmal $gp91^{phox}$ subunit to produce superoxide (Lambeth, 2004). In distinction, in endothelial cells, $p47^{phox}$ and $gp91^{phox}$ have an intracellular distribution, including the cytoskeleton and vesicular organelles, where ROS can be produced tonically or in response to an agonist (Li and Shah, 2002). In dissociated rat mNTS neurons, the potentiation of calcium currents induced by activation of the AT-1A receptor is mediated by ROS production via NADPH oxidase (Wang et al., 2004), however, the basal subcellular distribution of NADPH oxidase subunits in neurons of the mNTS is unknown. In addition to neurons, astrocytes, which are abundant in the mNTS, have also been shown to express functional NADPH oxidase (Abramov et al., 2005), however, the subcellular localization of phox proteins in NTS astroglia is also unknown.

Oxidation is an important modulator of catecholaminergic signaling pathways (Smythies and Galzigna, 1998). At intermediate and caudal levels, the mNTS contains many neurons that express tyrosine hydroxylase (TH), the rate-limiting enzyme in catecholamine biosynthesis (Zigmond et al., 1989). Catecholaminergic neurons in mNTS are sensitive to disturbance of cardiovascular (Chan et al., 1999), respiratory (Buller et al., 1999), fluid (Gordon et al., 1979), and metabolic (Willing and Berthoud, 1997) homeostasis. In addition, catecholamine containing axon terminals within the mNTS play an important modulatory role in the central regulation of systemic arterial pressure (Snyder et al., 1978). There is also an increase in TH activity in the NTS associated with rodent models of hypertension (Misu et al., 1995, Potts et al., 2000., Ferrari et al., 2002). The activity of TH is regulated by NADPH oxidase activation (Kuhn and Geddes, 2002), and by proteins associated with oxidative stress, such as nitrotyrosine (Kuhn et al., 2002). In addition, a major superoxide metabolite, hydrogen peroxide, is accessible to the extracellular milieu (Lambeth, 2004) and thus capable of influencing closely apposed structures. However, there is no evidence that NADPH oxidase subunits are present in TH containing neurons in the mNTS, or in astrocytes contacted by catecholamine containing axon terminals.

Immunogold electron microscopic cytochemistry has the spatial resolution necessary for the detection of protein immunolabeling at distinct subcellular localizations, and is also compatible with dual immunoperoxidase staining for related antigens. We used immunogold electron microscopy to determine the cellular and subcellular distributions of the $gp91^{phox}$ and $p47^{phox}$ subunits in neuronal and glial processes in the mNTS, at the level of the area postrema. To verify this distribution, immunogold labeling of the $p22^{phox}$ subunit was also determined in this brain region. Dual immunoperoxidase labeling for TH and immunogold detection of NADPH oxidase subunits was performed to determine whether catecholamine containing neurons also expressed $p47^{phox}$ or $gp91^{phox}$, or were apposed to NADPH oxidase subunit containing glia.

Materials and Methods

Subjects

Male Sprague-Dawley rats (Charles River) weighing 300–400 g were individually housed and maintained on a 12-hr light/dark cycle. All rats had unlimited access to water and rat chow in their home cages. The experimental protocols were carried out in accordance with the National Institute of Health Guide for the Care and Use of Laboratory Animals and were approved by the Institutional Animal Care and Use Committees at Weill Medical College of Cornell University. All efforts were made to minimize the number of animals used and their suffering.

Tissue preparation

Rats were anesthetized with sodium pentobarbital (150 mg/kg, i.p.), and their brains were fixed by aortic arch perfusion sequentially with: (a) 15 ml of normal saline (0.9%) containing 1000 units/ml of heparin, (b) 50 ml of 3.75% acrolein in 2% paraformaldehyde in 0.1 M phosphate buffer (PB, pH 7.4), and (c) 200 ml of 2% paraformaldehyde in PB, all delivered at a flow rate of 100 ml/minute. The brains were removed and post-fixed for 30 minutes in 2% paraformaldehyde in PB. Coronal sections 40 μm thick were cut with a vibrating microtome from brainstem at the level of the area postrema according to the atlas of Paxinos and Watson (1986). Tissue sections were next treated with 1.0% sodium borohydride in PB and then washed in PB. Sections then were immersed in a cryoprotectant solution (25% sucrose and 2.5% glycerol in 0.05 M PB) for 15 minutes. To enhance tissue permeability, sections were then freeze-thawed in liquid freon and liquid nitrogen. Sections were next rinsed in 0.1 M Tris-buffered saline (TS, pH 7.6) and then incubated for 30 minutes in 0.1% bovine serum albumin (BSA) to minimize nonspecific labeling.

Antisera

To immunolabel NADPH oxidase subunits, polyclonal goat anti-$p47^{phox}$, -$gp91^{phox}$, and -$p22^{phox}$ antisera (Santa Cruz Biotechnology, Santa Cruz, CA) were used. For dual labeling of $p47^{phox}$ and $gp91^{phox}$ a mouse anti- $gp91^{phox}$ antibody (BD Transduction Labs) was used in tandem with the goat anti- $p47^{phox}$ antisera in order to prevent species cross-reactivity. These antisera show recognition of their respective epitopes by Western Blotting, immunoprecipitation, and immunocytochemistry (Manufacturer's data). Preadsorption of each antisera with its respective blocking peptide prevented detection of immunolabeling (Wang et al., 2004). Catecholamine neurons were labeled with a well-characterized monoclonal mouse antibody raised against an epitope within the midportion of TH (ImmunoStar) (Glass et al., 2001). By western blotting, this monoclonal antibody does not cross-react with other major monoaminergic synthetic enzymes including dopamine-ß-hydroxylase, phenylethanolamine-N-methyltransferase, or tryptophan hydroxylase (Manufacturer's data). By light microscopy, immunolabeling of brain sections with this antisera produces labeling selectively in catecholaminergic cell groups, and deletion of the primary antibody produces no staining.

Immunocytochemical procedures

For single immunogold labeling of NADPH oxidase subunits, brainstem sections were incubated for 48 hours in separate solutions containing one of the phox antisera (1:50). Sections were rinsed in 0.01 M PBS (pH 7.4), and blocked for 10 minutes in 0.5% BSA and 0.1% gelatin in PBS to reduce non-specific binding of gold particles. Sections then were incubated for 2 hours in donkey anti-goat IgG conjugated with 1 nm gold particles (1:50, AuroProbeOne, Amersham, Arlington Heights, IL). The sections were rinsed in PBS and incubated for 10 minutes in 2% glutaraldehyde. The bound gold particles were enlarged by a 6 minute silver intensification using an IntenSE-M kit (Amersham, Arlington Heights, IL). Some sections were also processed for single immunoperoxidase labeling of NADPH oxidase subunits. Sections were incubated in primary antisera (1:100), and after incubation, were then rinsed in TS and prepared for peroxidase identification. Sections were incubated in anti-goat IgG conjugated to biotin, rinsed in TS, and then incubated for 30 minutes in avidin-biotin-peroxidase complex (1:100, Vectastain Elite Kit, Vector Laboratories) in TBS. The bound peroxidase was visualized by reaction for 5–6 minutes in 0.2% solution of 3, 3'-diaminobenzidine and 0.003% hydrogen peroxide in TS.

For dual detection of immunogold labeling of phox proteins and immunoperoxidase detection of TH, brainstem sections were incubated for 48 hours in a solution containing a mixture of either $p47^{phox}$ or $gp91^{phox}$ antisera (1:50) and the TH (1:25,000) antibody. After incubation, sections were rinsed in TS and prepared first for peroxidase identification of TH. Sections were incubated in anti-mouse IgG conjugated to biotin, rinsed in TS, and then incubated for 30 minutes in avidin-biotin-peroxidase complex (1:100, Vectastain Elite Kit, Vector Laboratories) in TBS. The bound peroxidase was visualized by reaction for 5–6 minutes in 0.2% solution of 3, 3'-diaminobenzidine and 0.003% hydrogen peroxide in TS. Sections were then processed for immunogold labeling. Sections were rinsed in 0.01 M PBS (pH 7.4), and blocked for 10 minutes in 0.5% BSA and 0.1% gelatin in PBS to reduce non-specific binding of gold particles. Sections then were incubated for 2 hours in donkey anti-goat IgG conjugated with 1 nm gold particles (1:50, AuroProbeOne, Amersham, Arlington Heights, IL). The sections were rinsed in PBS and incubated for 10 minutes in 2% glutaraldehyde. The bound gold particles were enlarged by a 6 minute silver intensification using an IntenSE-M kit (Amersham, Arlington Heights, IL). Alternate sections were processed for immunoperoxidase labeling of phox proteins (1:100) and immunogold detection of TH (1:4000). For dual labeling of NADPH oxidase subunits, goat anti-$p47^{phox}$ (1:50) and mouse anti-$gp91^{phox}$ (1:100) antisera were labeled by immunogold and immunoperoxidase methods, respectively. Each of the primary antisera was omitted during labeling conditions to determine the specificity of labeling. There

is the possibility that ABC/DAB reaction product will be intensified by silver enhancement. In our dual labeling experiments, the primary antisera labeled with a gold secondary was omitted as a control for this possibility (Chan et al., 1990). It should also be pointed out that even with the punctate immunoperoxidase staining frequently obtained when labeling for receptors and some other signaling proteins, the resultant reaction product is typically not particulate, but rather somewhat diffuse in nature, and thus with careful visual inspection not easily confused with silver enhanced immunogold.

For light microscopy, sections were mounted on glass slides, dehydrated, and covered in resin beneath a glass coverslip. For electron microscopy, sections were postfixed in 2% osmium tetroxide in PB for one hour, and dehydrated in a series of alcohols, through propylene oxide, and embedded in EM BED 812 (EMS, Fort Washington, PA) between 2 sheets of Aclar plastic. Ultrathin sections from the surface of the tissue were cut with a diamond knife using an ultramicrotome (Ultratome, NOVA, LKB, Bromma, Sweden). These sections were collected on grids, and then counterstained with Reynold's lead citrate and uranyl acetate.

Ultrastructural analysis

Electron microscopic sampling and analysis was conducted on a total of at least 62,500 μm^2 of thin sectioned mNTS sections obtained from no less than 6 animals. For the analysis of gold particle distributions, we used an established procedure that successfully shows regional differences in subcellular distribution of surface proteins in other brain regions (Haberstock-Debic et al., 2003). From the mNTS of each of three animals, two ultrathin sections at the tissue-surface interface were selected for analysis. Digital images were captured and analyzed to determine: (1) the number of labeled dendritic profiles, and (2) the number of gold-silver particles present in the cytoplasm, or in contact with the plasma membrane. Gold particles in contact with any portion of the surface membrane were considered as plasmalemmal. The classification of labeled dendrites was based upon descriptions by Peters et. al. (Peters et al., 1991). Dendrites were identified by the presence of postsynaptic densities, as well as ribosomes and both rough and smooth endoplasmic reticulum. However, profiles were also considered dendritic whenever postsynaptic densities were observed, independent of endoplasmic reticulum. Synapses were defined as either symmetric or asymmetric, according to the presence of either thin or thick postsynaptic specializations, respectively. Appositions were distinguished by closely spaced plasma membranes that lacked recognizable specializations, without the presence of interposing astrocytic processes. At least two gold-silver particles per profile were imposed as evidence of positive labeling in a neuropil in which comparable areas of epon, myelin or other tissues, not expected to express phox proteins, were largely devoid of gold-silver deposits. Under similar conditions of low background, we have recently shown that 1–2 gold particles in small profiles, such as dendritic spines, is equivalent to four or more in dendritic profiles with a larger surface area (Wang et al., 2003). Data were analyzed by t-tests, or one-or two-way factorial ANOVA, where applicable. For analysis of the ratio of plasmalemmal to surface immunogold labeling, the data were converted by arcsine prior to analysis to allow for comparison of proportions. Differences in means were analyzed by Fisher’s PLSD.

Light Microscopy

For light microscopy, the mounted sections were viewed with a Nikon Microphot-FX microscope (Nikon, Garden City, NY) equipped with a digital CoolSNAP camera (Photometrics, Huntington Beach, CA). The light microscopic images were acquired through an interface between the camera and a Macintosh computer. These images were adjusted for contrast and brightness using Photoshop 6.0 software, and imported into Powerpoint 2001, to add lettering and prepare the composite light microscopic figure.

Electron Microscopy

Electron microscopic images were using a digital camera (Advanced Microscopy Techniques) interfaced with a transmission electron microscope (Technai 12 BioTwin, FEI, Hillsboro, OR). For preparation of figures, images were adjusted for contrast and brightness using Photoshop 6.0 software, and imported into QuarkXpress 4.0, to add lettering. For quantification of cross-sectional area, surface area, as well as minor and major axis length digital images were analyzed with Microcomputer Imaging Device software (MCID, Imaging Research Inc., Ontario, Canada).

Results

In the dorsal vagal complex (Figure 1 top left) of brainstem sections processed for light microscopic single immunoperoxidase labeling for $p47^{phox}$ (Figure 1), there were apparent neuronal somata showing staining within the mNTS (Fig.1 bottom). In addition, there were many instances of elongated processes, which were frequently present near blood vessels (not shown). A similar labeling pattern was seen for the other NADPH oxidase subunits (data not shown).

Electron microscopic imaging of single $p47^{phox}$ immunogold labeled profiles in the mNTS

Within the mNTS, immunogold labeling of $p47^{phox}$ was present in somata and dendritic profiles. Within somata, $p47^{phox}$ was frequently present in association with rough endoplasmic reticula (rER) and round vesicular organelles (Fig. 2A). Less frequently, $p47^{phox}$ immunogold particles were present near the plasmalemma of these cell bodies. Within dendritic profiles, immunogold-silver deposits for $p47^{phox}$ were often associated with intracellular organelles, particularly endomembrane-like tubular organelles characteristic of smooth endoplasmic reticula (sER) (Fig. 2B). Immunolabeled dendrites were present in the neuropil as well as near the neurovasculature (Fig. 2B). Immunogold particles for $p47^{phox}$ were also frequently found in association with the surface membrane of dendritic profiles when labeled with immunogold (Fig. 2C) or immunoperoxidase methods (Fig. 2D).

Immunogold labeling for $p47^{phox}$ was also frequently present in non-neuronal compartments, particularly astrocytes. Immunogold-silver deposits were present in the cell bodies of astrocytes, often in association with Golgi complexes (GC) and small round vesicular organelles (Fig. 3A). More frequently, however, immunogold particles for $p47^{phox}$ were found in thin elongated processes present within the neuropil (Fig. 3B). These small astrocytic profiles frequently surrounded unlabeled axons or dendrites, many of which formed appositions or synapses. In addition, $p47^{phox}$ immunolabeling was often present in perivascular astrocytes. In these processes, $p47^{phox}$ immunogold labeling was conspicuously present beneath the surface membrane in contact with the basal lamina (Fig. 3C).

Electron microscopic imaging of $gp91^{phox}$ immunogold labeling in the mNTS

Within the mNTS, $gp91^{phox}$ immunogold labeling was present in both neuronal and glial profiles. Similar to what was described for $p47^{phox}$, immunogold-silver deposits for $gp91^{phox}$ were found in Golgi complexes and the rER of neuronal somata (Fig. 4A). Dendritic profiles containing $gp91^{phox}$ immunolabeling were present within the neuropil containing unlabeled small unmyelinated axons and axon terminals (Fig. 4B). Within these dendrites, gold-silver deposits for $gp91^{phox}$ were present near the surface membrane (Fig. 4B) as well as vesicular organelles (Fig. 4B) and mitochondria (Fig. 4C). Labeling near the surface membrane and vesicular organelles was also seen with an immunoperoxidase marker (Fig. 4D). Labeling for $gp91^{phox}$ was also present in the cell bodies of astrocytes (Fig. 5A) where immunogold particles were frequently located near Golgi complexes and vesicular organelles, while sporadic labeling near fibers was also seen. Gold-silver deposits were also seen in small glial

processes within the neuropil containing phox labeled dendritic profiles (Fig. 5B). Small elongated gp91^{phox} labeled glial processes were also often present in the neuropil when labeled for immunoperoxidase detection (Fig. 5C).

Dual electron microscopic imaging of p47^{phox} and gp91^{phox} labeling in the mNTS

Since functional NADPH oxidase requires the formation of a p47^{phox} - gp91^{phox} complex, brainstem sections were also processed for dual immunogold and immunoperoxidase labeling for these proteins, respectively. In the mNTS, immunogold and immunoperoxidase reaction product for these proteins were sometimes found in separate subcellular sites, but were also frequently found to overlap. In dendritic profiles aggregates of immuoperoxidase reaction product for gp91^{phox} were present near endosomal-like vesicular organelles that also contained immunogold-silver deposits for p47^{phox} (Fig. 6A). In addition, overlapping phox protein immunolabeling was also present in intracellular sites near mitochondria (Fig. 6B) or near the surface membrane of dendritic profiles (Fig. 6C). Similarly, profiles of small astrocytic processes also showed overlapping gp91^{phox} and p47^{phox} immunoreactivity (Fig. 6D).

Electron microscopic imaging of p22^{phox} immunogold labeling in the mNTS

Separate brainstem sections were processed for single immunogold labeling of p22^{phox}. Similar to the observed immunogold labeling of p47^{phox} and gp91^{phox}, the p22^{phox} subunit was present in somata and dendritic profiles in mNTS neurons. Gold labeling of p22^{phox} was also frequently present in association with Golgi complexes and small round vesicular organelles in somata (Fig. 7A). Immunogold labeling was also found in intracellular sites including mitochondria in large dendritic profiles that were apposed by unlabeled axon terminals (Fig. 7B). In addition, p22^{phox} immunolabeling was also present near the surface membrane of small dendritic profiles that were contacted by unlabeled axon terminals (Fig. 7C). p22^{phox} labeled dendrites were also frequently seen near the neurovasculature (Fig. 7D). Compared to the other phox proteins, there was also a comparable degree of p22^{phox} labeling in astrocytic processes. Within the cell bodies of glia, single immunogold particles were present in association with Golgi complexes and vesicular organelles (Fig. 8A), whereas in small astrocytic processes p22^{phox} formed aggregates near vesicular organelles (Fig. 8B). During the course of visual inspection of sampled tissue, numerous phox labeled astrocytic profiles were observed near the neurovasculature, frequently on the surface membrane apposed to the basal lamina (Fig. 8C), although these relationships were not quantified.

Quantification of phox proteins in neuronal or astrocytic compartments in the mNTS

The majority of p47^{phox} immunogold labeled profiles were cell bodies (n=92), dendrites (n=216) or glial processes (n=236), only a small number were axons (n=26) or axon terminals (n=26; Fig. 9A). In addition, most of the gp91^{phox} immunogold labeled profiles were cell bodies (n=45), dendrites (n=162) or glial processes (n=199), only a small number were axons (n=3) or axon terminals (n=13; Fig. 9B). Similar to the other phox proteins, p22^{phox} was present to a higher degree in dendrites (n=72), soma (n=23), and glia (n=74), and to a much lesser extent axon terminals (n=16) and axons (n=3 ; Fig. 9C).

Comparison of subcellular p47^{phox} and gp91^{phox} gold labeling in mNTS neurons and astrocytes

Morphometric comparison of p47^{phox} and gp91^{phox} immunolabeled dendritic profiles indicated that there were no differences in the cross-sectional (2.3±.29 μm versus 2.2±.36 μm, p=.93) or surface (5.8±.4 versus 5.8±.5, p=.96) areas between each group of processes. There was also no difference in the total number of gold particles in p47^{phox} or gp91^{phox} labeled dendritic profiles (2.8±.16 versus 2.5±.2, p=.25). In addition, the intracellular distribution of p47^{phox} or gp91$^{phox\ in}$ mNTS labeled dendritic processes was comparable (p=.89; Fig. 10A)

(Table 1A). When gold labeling was categorized by type of intracellular organelle, there were still no differences in cytosolic (p=.9), vesicular (p=.5) or mitochondrial (p=.24) labeling (Table 1A). There was, however, a significantly higher frequency of dendritic plasmalemmal immunogold labeling of $p47^{phox}$ as compared to $gp91^{phox}$ in the mNTS (p=.04; Table 1A; Fig 10B).

In glial profiles, there were no differences in total (5.0±.5 versus 6.7±.8, p=.08), intracellular (p=.09), or surface (p=.6) immunogold labeling of $p47^{phox}$ or $gp91^{phox}$ in the mNTS (Table 1B). When intracellular gold labeling was categorized by type of intracellular organelle, there were significant differences in phox protein labeling in mNTS glia. There was a higher incidence of $p47^{phox}$ labeling in the cytosol (p<.05, Fig. 11) compared to $gp91^{phox}$. However, there was a significantly higher number of $gp91^{phox}$ gold particles in association with vesicular organelles as compared to $p47^{phox}$ (p=.03; Table 1B, Fig. 11).

Electron microscopic imaging of $p47^{phox}$ immunogold and TH immunoperoxidase labeled profiles in the mNTS

Immunogold-silver deposits for $p47^{phox}$ were found in somatodendritic profiles that also contained immunoperoxidase reaction product for the catecholamine synthesizing enzyme TH. Similar to single labeled profiles, $p47^{phox}$ immunolabeling was often present near Golgi complexes and rER of cell bodies also labeled for TH (Fig. 12A). Further, gold particles were also frequently seen near vesicular organelles and the surface membrane in catecholaminergic dendritic profiles (Fig. 12B). In addition to colocalization with TH in neurons, $p47^{phox}$ was seen in thin elongated glial processes that were apposed to TH immunolabeled axons or axon terminals (Fig. 12C).

Quantification of $p47^{phox}$ immunogold and TH immnoperoxidase labeling in the mNTS

Of all TH immunoreactive somata or dendrites, approximately 21% (73/339) also showed labeling for $p47^{phox}$, whereas approximately 24% (73/308) of $p47^{phox}$ profiles were labeled for TH. In addition, there were many instances of appositions between $p47^{phox}$ labeled somatodendritic profiles or glia and TH labeled axons or axon terminals. Approximately 10% (25/236) of all $p47^{phox}$ labeled glia and 26% (81/308) of somatodendrites were apposed by TH immunoreactive axons.

Electron microscopic imaging of $gp91^{phox}$ immunogold and TH immunoperoxidase labeled profiles in the mNTS

Within the mNTS, $gp91^{phox}$ immunoreactivity was frequently present in neurons immunolabeled for TH. In somatodendritic profiles that contained immunoperoxidase reaction product for the catecholamine synthesizing enzyme, $gp91^{phox}$ immunogold particles were often present near vesicular organelles or the surface membrane (Fig. 13A). Dendritic profiles containing $gp91^{phox}$ were sometimes apposed by axon terminals containing TH (Fig. 13B). In addition to colocalization with TH in neurons, $gp91^{phox}$ was often located in thin elongated glial processes that were apposed to TH immunolabeled axons or axon terminals (Fig. 13C).

Quantification of $gp91^{phox}$ immunogold and TH immnoperoxidase labeling in the mNTS

In tissue processed for dual labeling, approximately 76% (58/76) of all TH labeled somatodendritic profiles were also immunoreactive for $gp91^{phox}$, and approximately 28% (58/207) of all $gp91^{phox}$ somatodendrites were also labeled for TH. Approximately 10% (20/207) of all labeled somatodendrites, and 3% (6/199) of all $gp91^{phox}$ labeled glia and were apposed by TH immunoreactive axons.

Discussion

The present study provides the first immunocytochemical evidence that $p47^{phox}$, $gp91^{phox,}$ and $p22^{phox}$ are present in neuronal and astrocytic processes in the rat mNTS. Immunolabeling of each NADPH oxidase subunit was predominantly present in somatodendritic profiles as well as perineuronal and perivascular astrocytic processes. These results, in conjunction with overlapping $p47^{phox}$ and $gp91^{phox}$ immunolabeling, suggest that NADPH oxidase mediated superoxide production in the mNTS is likely to impact postsynaptic responses of neurons, as well as the activity of glia. In addition, many mNTS neurons were dually labeled for phox proteins and TH, while many catecholaminergic axons frequently apposed phox labeled astrocytes. Thus, of the many neuronal phenotypes present in the mNTS, catecholaminergic neurons are likely to play a significant role in the actions of superoxide produced by NADPH oxidase.

Somatodendritic labeling of phox proteins in mNTS neurons

Within the mNTS, immunogold labeling of $p47^{phox}$, $gp91^{phox}$, or $p22^{phox}$ was present in somata and dendrites. Within somata, phox protein immunoreactivity was associated with intracellular organelles that are involved in protein synthesis and transport, including rER and Golgi complexes. NADPH oxidase subunit labeling was also found near mitochondria as well as the surface membrane in cell bodies. Thus, the subcellular distribution of phox proteins as revealed by immunogold labeling is consistent with active synthesis and transport within mNTS neuronal somata, as also shown in non-neuronal cell types (Yu et al., 1999).

Within dendritic profiles, NADPH oxidase subunit immunolabeling was frequently found in intracellular sites, including small tubulovesicular organelles and mitochondria. The tubulovesicular organelles exhibited the morphology of smooth ER, some of which were also associated with the outer mitochondrial membrane. Phox immunolabeling in dendritic smooth ER, known sites for storage and intracellular release of calcium, provides ultrastructural evidence for the regulation of calcium levels in mNTS neurons by superoxide produced by NADPH oxidase (Wang et al., 2004, Kimura et al., 2005). In addition to intracellular sites, phox protein immunolabeling was also seen at synaptic and peri-synaptic areas of the plasmalemma. This is in accord with previous findings that NADPH oxidase has a synaptic distribution in other brain regions (Tejada-Simon et al., 2005).

Phox proteins in mNTS neurons: Functional considerations

Production of ROS within central autonomic circuitry is emerging as an important substrate of neural cardiovascular regulation (Wang et al., 2004). Our ultrastructural evidence for phox labeling in association with membranous organelles, including endoplasmic reticula, is in agreement with physiological results indicating that the potentiation of calcium currents induced by AT-1A receptor activation is mediated by NADPH dependent superoxide production in mNTS neurons (Wang et al., 2004). Together these findings suggest that superoxide production and increased calcium levels induced by AT-1A receptor activation in mNTS neurons occurs near diverse cellular membranes, including the plasmalemma and endoplasmic reticula. Thus, one cellular mechanism by which ROS production may modulate the activity of mNTS neurons is by redox regulation of cell surface or endomembrane proteins (Wolin, 2004), leading to increased intracellular calcium. Thus, within the mNTS, NADPH oxidase-induced superoxide production may be an important link between extracellular signals, such as ANGII, and intracellular events related to calcium signaling.

Astroglial labeling of phox proteins in mNTS

In addition to neurons, mNTS glia were also frequently immunoreactive for NADPH oxidase subunits. The larger glial processes had the morphology of fibrous astrocytes, as indicated by

ovoid nuclei, the presence of dense glial fibrillary acidic protein-like fibers within the cytosol of cell bodies, the latter of which gave off small thin organelle-sparse processes that traversed the surrounding neuropil (Peters et al., 1991). Within astrocytic somata, immunogold particles for phox proteins were associated with Golgi complexes and rough ER. In the thin processes, gold particles for NADPH oxidase subunits often formed aggregates near the outer membrane of vesicular organelles. Phox protein immunolabeling was also frequently observed in association with the plasma membrane of small astrocytic profiles that were apposed to unlabeled or phox labeled dendritic profiles or axons. In addition, glial profiles showing NADPH oxidase subunit labeling were often present near blood vessels. When present near the vasculature, immunolabeling for phox proteins was mainly located on the surface membrane apposed to other glia, or beneath the basal lamina beneath endothelial or smooth muscle cells. The finding that NADPH oxidase subunit labeling is prominent in astrocytes of the mNTS is consistent with a number of recent reports providing evidence for astrocytic phox proteins in other brain regions (Abramov et al., 2005).

Phox proteins in mNTS astrocytes: Functional considerations

Astrocytes are emerging as an important component of neural autonomic regulatory circuits. For example, astrocytes are the primary source of angiotensinogen in brain autonomic pathways, and are thus a crucial component of the central renin-angiotensin system (Morimoto et al., 2001). In addition, systemic hypertension is associated with increased mNTS angiotensinogen (Sangaleti et al., 2004) and brain ROS (Zimmerman and Davisson, 2004), whereas expression of the angiotensinogen gene is regulated by factors known to be sensitive to ROS production (Agarwal et al., 2004). These findings, together with the present results, suggest that mNTS astrocytes may couple hypertension with oxidative stress and ANGII activity.

Many of the astrocytes labeled for phox proteins were present in association with the neurovasculature. These labeled astroglia were often found in close proximity to endothelial cells, frequently in direct contact with the basal lamina. Thus, NADPH oxidase activation may be sensitive to circulating or endothelial derived factors, including ANGII or nitric oxide (NO) produced by endothelial nitric oxide synthase (eNOS). In addition to ANGII, NO produced by eNOS is a known neuromodulator of cardiovascular processes by acting on mNTS baroreflex circuitry (Paton et al., 2001). The close coupling of phox proteins with neurovascular structures in the mNTS suggests that NADPH oxidase-induced superoxide production is strategically targeted for the modulation of signals derived from endothelial cells, astrocytes, and the adjacent neuropil.

Tyrosine hydroxylase and phox proteins in neurons and astrocytes in mNTS

Within the mNTS, $p47^{phox}$ and $gp91^{phox}$ proteins were often co-localized with TH in somatodendritic processes. NADPH oxidase subunits were present in somata showing various intensities of immunoperoxidase reaction product for TH. However, phox labeling was independent of the levels of TH labeling in somata, where it was frequently present in association with rER, Golgi complexes, and endomembrane organelles. The presence of NADPH oxidase subunit labeling in TH containing neurons that are also known to express the alpha-2A adrenergic receptor (Glass et al., 2001) or the AT-1A receptor (Glass et al., 2005.) indicates that superoxide production may play a role in catecholamine and angiotensin signaling in mNTS neurons.

Phox protein immunolabeled astrocytic profiles were frequently apposed to TH immunoreactive dendrites and axons in the mNTS. Glial cells of similar morphology to those currently described, have been shown to contain surface and intracellular adrenergic receptors (Glass et al., 2001). In addition, the extraneuronal monoamine transporter expressed in glia is

known to be present in high density within the brainstem, suggesting that NADPH oxidase subunit labeled glia apposed to TH expressing neurons are capable of catecholamine binding and uptake.

Tyrosine hydroxylase and phox proteins in mNTS neurons and glia: Functional Considerations

It is known that TH is sensitive to cardiorespiratory and other forms of stress (Chan and Sawchenko, 1995, Chan and Sawchenko, 1998). In addition, free radicals can modulate the activity of TH (Kuhn and Geddes, 2002, Kuhn et al., 2002), while the oxidation of catecholamines, such as norepinephrine, results in reactive molecules that impact a variety of intracellular processes including mitochondrial respiration and regulation of metabolic enzymes (Xin et al., 2000). It is also important to note that hydrogen peroxide, a major superoxide metabolite, is accessible to the extracellular milieu (Lambeth, 2004) and thus may influence closely apposed structures. Thus, catecholamine signaling in the mNTS, which is known to play a role in the regulation of systemic arterial pressure (Snyder et al., 1978), may be directly modulated by superoxide generated by NADPH oxidase in neurons, or indirectly in apposed astroglia.

NADPH oxidase subunit localization in the mNTS: Conclusions

The subcellular localization of NADPH oxidase-mediated superoxide production has important consequences for intracellular signaling (Lambeth, 2004). Within the framework of the classic neutrophil model, the basally quiescent NADPH oxidase requires stimulation for assembly and superoxide production at the surface membrane. However the precise spatial location of active phox proteins is now known to depend upon cellular phenotype. For example, in endothelial cells functional NADPH oxidase is present intracellularly, frequently in association with the perinuclear cytoskeleton, where it also produces ROS at low basal levels (Li and Shah, 2002). The present results demonstrate that phox subunits in mNTS neurons and astroglia are present near the surface membrane, as well as near endoplasmic reticula-like vesicular organelles, known sites for storage and release of intracellular calcium. These findings therefore indicate further cell phenotypic diversity of NADPH oxidase function. In addition, the presence of phox proteins in diverse cellular compartments of mNTS neurons and glia supports a structural basis for the emerging role of redox modulation of autonomic, and particularly cardiovascular processes. Moreover, given the important role of ROS, dorsal vagal pathology, and autonomic dysfunction in neurological disease, aberrant free radical production in the NTS may be a potential candidate substrate of dorsal vagal damage accompanying sudden infant death syndrome (Sparks et al., 1996, Biondo et al., 2004), myocardial infarction (De Caro et al., 2000), as well as several major neurological disorders (Saper et al., 1991, Schroder and Linke, 1999, Dewey, 2004).

Acknowledgements

This work is supported by NIH grant HL18974

References

Abramov AY, Jacobson J, Wientjes F, Hothersall J, Canevari L, Duchen MR. Expression and modulation of an NADPH oxidase in mammalian astrocytes. J Neurosci 2005;25:9176–9184. [PubMed: 16207877]

Agarwal R, Campbell RC, Warnock DG. Oxidative stress in hypertension and chronic kidney disease: role of angiotensin II. Seminars in Nephrology 2004;24:101–114. [PubMed: 15017522]

Agassandian K, Fazan VP, Margaryan N, Dragon DN, Riley J, Talman WT. A novel central pathway links arterial baroreceptors and pontine parasympathetic neurons in cerebrovascular control. Cell Mol Neurobiol 2003;23:463–478. [PubMed: 14514008]

Aicher SA, Milner TA, Pickel VM, Reis DJ. Anatomical substrates for baroreflex sympathoinhibition in the rat. Brain Res Bull 2000;51:107–110. [PubMed: 10709955]

Barraco, IRA., editor. Nucleus of the Solitary Tract. CRC; Boca Raton: 1994.

Biondo B, Magagnin S, Bruni B, Cazzullo A, Tosi D, Matturri L. Glial and neuronal alterations in the nucleus tractus solitarii of sudden infant death syndrome victims. Acta Neuropathologica 2004;108:309–318. [PubMed: 15300449]

Buller KM, Smith DW, Day TA. NTS catecholamine cell recruitment by hemorrhage and hypoxia. Neuroreport 1999;10:3853–3856. [PubMed: 10716222]

Cai H, Griendling KK, Harrison DG. The vascular NAD(P)H oxidases as therapeutic targets in cardiovascular diseases. Trends Pharmacol Sci 2003;24:471–478. [PubMed: 12967772]

Campese VM, Ye S, Zhong H, Yanamadala V, Ye Z, Chiu J. Central ROS play a role in regulation of systemic blood pressure, possibly by modulating SNS activity. Am J Physiol 2004;287:H695–703.

Chan J, Aoki C, Pickel VM. Optimization of differential immunogold-silver and peroxidase labeling with maintenance of ultrastructure in brain sections before plastic embedding. J Neurosci Methods 1990;33:113–127. [PubMed: 1977960]

Chan JY, Chen WC, Lee HY, Chang TJ, Chan SH. Phosphorylation of transcription factor cyclic-AMP response element binding protein mediates c-fos induction elicited by sustained hypertension in rat nucleus tractus solitarii. Neurosci 1999;88:1199–1212.

Chan RKW, Sawchenko PE. Hemodynamic regulation of tyrosine hydroxylase messenger RNA in medullary catecholamine neurons: a c-fos-guided hybridization histochemical study. Neurosci 1995;66:377–390.

Chan RKW, Sawchenko PE. Differential time- and dose-related effects of haemorrhage on tyrosine hydroxylase and neuropeptide Y mRNA expression in medullary catecholamine neurons. Eur J Neurosci 1998;10:3747–3758. [PubMed: 9875353]

Chan SH, Hsu KS, Huang CC, Wang LL, Ou CC, Chan JY. NADPH oxidase-derived superoxide anion mediates angiotensin II-induced pressor effect via activation of p38 mitogen-activated protein kinase in the rostral ventrolateral medulla. Circulation Res 2005;97:772–780. [PubMed: 16151022]

De Caro R, Parenti A, Montisci M, Guidolin D, Macchi V. Solitary tract nuclei in acute heart failure. Stroke 2000;31:1187–1193. [PubMed: 10797184]

Dewey RB. Autonomic dysfunction in Parkinson's disease. Neurologic Clinics 2004;22(3 Suppl):S127–139. [PubMed: 15501361]

Diz DI, Westwood B, Averill DB. AT(1) antisense distinguishes receptors mediating angiotensin II actions in solitary tract nucleus. Hypertension 2001;37:1292–1297. [PubMed: 11358943]

Ferrari MF, Almeida RS, Chadi G, Fior-Chadi DR. Acute changes in 3H-PAC and 125I-PYY binding in the nucleus tractus solitarii and hypothalamus after a hypertensive stimulus. Clinical Experimental Hypertension 2002;24:169–186.

Glass MJ, Briggs JE, Billington CJ, Kotz CM, Levine AS. Opioid receptor blockade in rat nucleus tractus solitarius alters amygdala dynorphin gene expression. Am J Physiol 2002;283:R161–167.

Glass MJ, Huang J, Aicher SA, Milner TA, Pickel VM. Subcellular localization of alpha-2A-adrenergic receptors in the rat medial nucleus tractus solitarius: regional targeting and relationship with catecholaminergic neurons. J Comp Neurol 2001;433:193–207. [PubMed: 11283959]

Glass MJ, Huang J, Speth RC, Iadecola C, Pickel VM. Angiotensin II AT-1A receptor immunolabeling in rat medial nucleus tractus solitarius neurons: subcellular targeting and relationships with catecholamines. Neurosci 2005;130:713–723.

Gordon FJ, Brody MJ, Fink GD, Buggy J, Johnson AK. Role of central catecholamines in the control of blood pressure and drinking behavior. Brain Res 1979;178:161–173. [PubMed: 497858]

Gozal D, Gozal E, Simakajornboon N. Signaling pathways of the acute hypoxic ventilatory response in the nucleus tractus solitarius. Respiration Physiol 2000;121:209–221.

Haberstock-Debic H, Wein M, Barrot M, Colago EE, Rahman Z, Neve RL, Pickel VM, Nestler EJ, von Zastrow M, Svingos AL. Morphine acutely regulates opioid receptor trafficking selectively in dendrites of nucleus accumbens neurons. J of Neurosci 2003;23:4324–4332. [PubMed: 12764121]

Kim-Mitsuyama S, Yamamoto E, Tanaka T, Zhan Y, Izumi Y, Izumiya Y, Ioroi T, Wanibuchi H, Iwao H. Critical role of angiotensin II in excess salt-induced brain oxidative stress of stroke-prone spontaneously hypertensive rats. Stroke 2005;36:1083–1088. [PubMed: 15817892]

Kimura S, Zhang G, Nishiyama A, Shokoji T, Yao L, Fan Y, Rahman M, Suzuki T, Maeta H, Abe Y. Role of NAD(P)H Oxidase- and Mitochondria-Derived Reactive Oxygen Species in Cardioprotection of Ischemic Reperfusion Injury by Angiotensin II. Hypertension 2005;45:860–866. [PubMed: 15824196]

Kuhn DM, Geddes TJ. Reduced nicotinamide nucleotides prevent nitration of tyrosine hydroxylase by peroxynitrite. Brain Res 2002;933:85–89. [PubMed: 11929639]

Kuhn DM, Sadidi M, Liu X, Kreipke C, Geddes T, Borges C, Watson JT. Peroxynitrite-induced nitration of tyrosine hydroxylase: identification of tyrosines 423, 428, and 432 as sites of modification by matrix-assisted laser desorption ionization time-of-flight mass spectrometry and tyrosine-scanning mutagenesis. J Biol Chem 2002;277:14336–14342. [PubMed: 11834745]

Lambeth JD. Nox enzymes and the biology of reactive oxygen. Nat Rev Immunol 2004;4:181–189. [PubMed: 15039755]

Lassègue B, Clempus RE. Vascular NAD(P)H oxidase specific features, expression, and regulation. Am J Physiol 2003;285:R277–R297.

Lawrence AJ, Jarrott B. Neurochemical modulation of cardiovascular control in the nucleus tractus solitarius. Prog Neurobiol 1996;48:21–53. [PubMed: 8830347]

Li JM, Shah AM. Intracellular localization and preassembly of the NADPH oxidase complex in cultured endothelial cells. J Biol Chem 2002;277:19952–19960. [PubMed: 11893732]

Mayorov DN, Head GA, De Matteo R. Tempol attenuates excitatory actions of angiotensin II in the rostral ventrolateral medulla during emotional stress. Hypertension 2004;44:101–106. [PubMed: 15159379]

Misu Y, Yue JL, Okumura Y, Miyamae T, Ueda H. Altered basal release and depressor effect of L-DOPA in the nucleus tractus solitarii of spontaneously hypertensive rats. Clin Exper Pharmacol Physiol 1995;22:S34–36.

Morimoto S, Cassell MD, Beltz TG, Johnson AK, Davisson RL, Sigmund CD. Elevated blood pressure in transgenic mice with brain-specific expression of human angiotensinogen driven by the glial fibrillary acidic protein promoter. Circulation Research 2001;89:365–372. [PubMed: 11509454]

Paton JF, Deuchars J, Ahmad Z, Wong LF, Murphy D, Kasparov S. Adenoviral vector demonstrates that angiotensin II-induced depression of the cardiac baroreflex is mediated by endothelial nitric oxide synthase in the nucleus tractus solitarii of the rat. J Physiol 2001;531:445–458. [PubMed: 11230517]

Peters, A.; Palay, SL.; Webster, H. The fine structure of the nervous system. Oxford University Press; New York: 1991.

Potts PD, Ludbrook J, Gillman-Gaspari TA, Horiuchi J, Dampney RA. Activation of brain neurons following central hypervolaemia and hypovolaemia: contribution of baroreceptor and non-baroreceptor inputs. Neurosci 2000;95:499–511.

Sangaleti CT, Crescenzi A, Michelini LC. Endogenous angiotensin and pressure modulate brain angiotensinogen and AT1A mRNA expression. Hypertension 2004;43:317–323. [PubMed: 14732738]

Saper CB, Sorrentino DM, German DC, de Lacalle S. Medullary catecholaminergic neurons in the normal human brain and in Parkinson's disease. Annals of Neurology 1991;29:577–584. [PubMed: 1892359]

Schroder R, Linke RP. Cerebrovascular involvement in systemic AA and AL amyloidosis: a clear haematogenic pattern. Virchows Archiv 1999;434:551–560. [PubMed: 10394892]

Serrano F, Kolluri NS, Wientjes FB, Card JP, Klann E. NADPH oxidase immunoreactivity in the mouse brain. Brain Res 2003;988:193–198. [PubMed: 14519542]

Smythies J, Galzigna L. The oxidative metabolism of catecholamines in the brain: a review. Biochimica et Biophysica Acta 1998;1380:159–162. [PubMed: 9565677]

Snyder DW, Nathan MA, Reis DJ. Chronic lability of arterial pressure produced by selective destruction of the catecholamine innervation of the nucleus tractus solitarii in the rat. Circ Res 1978;43:662–671. [PubMed: 688565]

Sparks DL, Davis DG, Bigelow TM, Rasheed K, Landers TM, Liu H, Coyne CM, Hunsaker JC. Increased ALZ-50 immunoreactivity in sudden infant death syndrome. J of Child Neurol 1996;11:101–107. [PubMed: 8881985]

Sumimoto H, Miyano K, Takeya R. Molecular composition and regulation of the Nox family NAD(P)H oxidases. Biochem Biophys Res Comm 2005;338:677–686. [PubMed: 16157295]

Taniyama Y, Griendling KK. Reactive oxygen species in the vasculature: molecular and cellular mechanisms. Hypertension 2003;42:1075–1081. [PubMed: 14581295]

Tejada-Simon MV, Serrano F, Villasana LE, Kanterewicz BI, Wu G, Quinn MT, Klann E. Synaptic localization of a functional NADPH oxidase in the mouse hippocampus. Mol Cell Neurosci 2005;29:97–106. [PubMed: 15866050]

Vallet P, Charnay Y, Steger K, Ogier-Denis E, Kovari E, Herrmann F, Michel JP, Szanto I. Neuronal expression of the NADPH oxidase NOX4, and its regulation in mouse experimental brain ischemia. Neurosci 2005;132:233–238.

Wang G, Anrather J, Huang J, Speth RC, Pickel VM, Iadecola C. NADPH oxidase contributes to angiotensin II signaling in the nucleus tractus solitarius. J Neurosci 2004;24:5516–5524. [PubMed: 15201324]

Wang H, Cuzon VC, Pickel VM. Postnatal development of mu-opioid receptors in the rat caudate-putamen nucleus parallels asymmetric synapse formation. Neurosci 2003;118:695–708.

Willing AE, Berthoud HR. Gastric distension-induced c-fos expression in catecholaminergic neurons of rat dorsal vagal complex. Am J Physiol 1997;272:R59–R67. [PubMed: 9038991]

Wolin MS. Subcellular localization of Nox-containing oxidases provides unique insight into their role in vascular oxidant signaling. Arteriosclerosis, Thrombosis and Vascular Biology 2004;24:625–627.

Xin W, Shen XM, Li H, Dryhurst G. Oxidative metabolites of 5-S-cysteinylnorepinephrine are irreversible inhibitors of mitochondrial complex I and the alpha-ketoglutarate dehydrogenase and pyruvate dehydrogenase complexes: possible implications for neurodegenerative brain disorders. Chem Res Toxicol 2000;13:749–760. [PubMed: 10956063]

Yu L, DeLeo FR, Biberstine-Kinkade KJ, Renee J, Nauseef WM, Dinauer MC. Biosynthesis of flavocytochrome b558. gp91(phox) is synthesized as a 65-kDa precursor (p65) in the endoplasmic reticulum. J Biol Chem 1999;274:4364–4369. [PubMed: 9933639]

Zigmond RE, Schwarzschild MA, Rittenhouse AR. Acute regulation of tyrosine hydroxylase by nerve activity and by neurotransmitters via phosphorylation. Annu Rev Neurosci 1989;12:415–461. [PubMed: 2564757]

Zimmerman MC, Davisson RL. Redox signaling in central neural regulation of cardiovascular function. Prog Biophysics Mol Biol 2004;84:125–149.

Zimmerman MC, Sharma RV, Davisson RL. Superoxide mediates angiotensin II-induced influx of extracellular calcium in neural cells. Hypertension 2005;45:717–723. [PubMed: 15699459]

LIST OF ABBREVIATIONS USED IN MAIN TEXT

ABC
avidin biotin peroxidase complex

ANGII
Angiotensin II

AT-1A
Angiotensin II receptor subtype 1A

AP
area postrema

BSA
bovine serum albumin

GC
Golgi complex

IgG
immunoglobulin G

m

mitochondria

mNTS
medial nucleus of the solitary tract

NADPH
oxidase nicotinamide adenine dinucleotide phosphate-oxidase

PB
phosphate buffer

PBS
phosphate-buffered saline

phox
phagocyte oxidase

RAC
Rho-related C3 botulinum toxin substrate

ROS
reactive oxygen species

rER
rough endoplasmic reteicula

sER
smooth endoplasmic reteicula

sol
solitary tract

TH
tyrosine hydroxylase

TS
Tris-buffered saline

vo
vesicular orgenelle

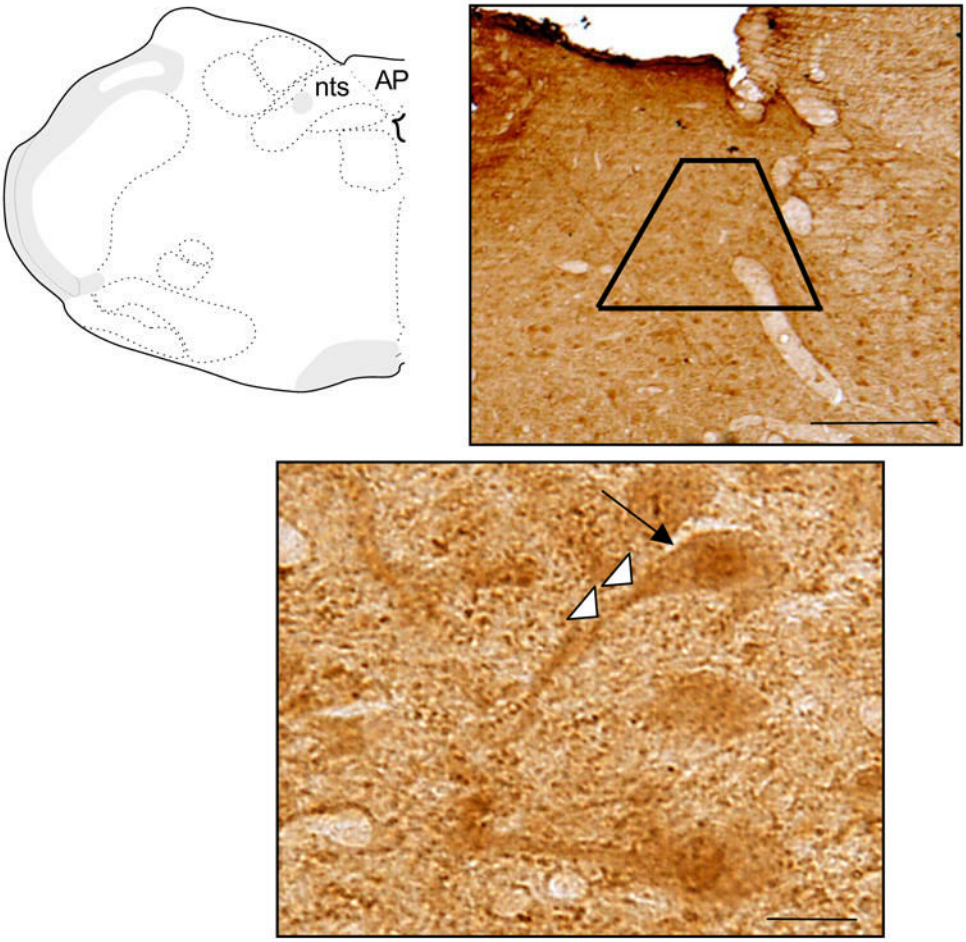

Figure 1.

Light microscopic immunoperoxidase labeling for p47^{phox} in the dorsal vagal complex. At the top left, a schematic figure representing the brainstem level sampled in the present study is provided for orientation. At the top right, p47^{phox} immunoperoxidase labeling in the mNTS and adjacent dorsal motor nucleus and area postrema are shown in a 40 μm coronal section through the dorsal medulla. The trapezoid illustrates the relative size and location of the area in which ultrathin sections were obtained for electron microscopic analysis in separately processed brainstem sections. A high power light micrograph shows a neuron (large arrow) with immunoperoxidase labeling for p47^{phox} in the soma and primary dendrite (small white arrows). AP= area postrema, nts= nucleus of the solitary tract. Scale bars = 0.5 mm (top), 10 μm (bottom).

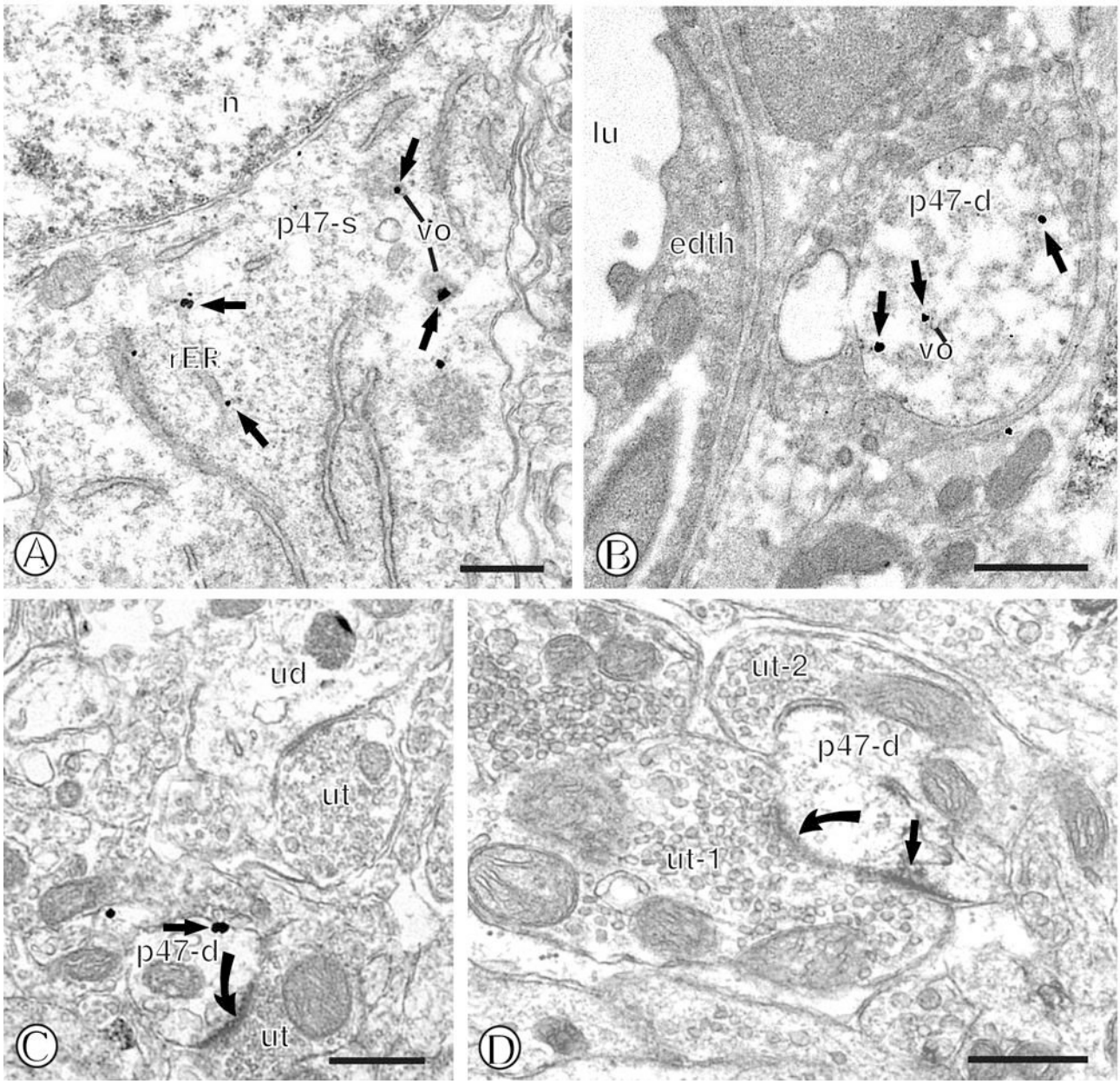

Figure 2.

Immunogold labeling of p47^{phox} in mNTS neurons. (A). Immunogold particles (small closed arrows) for p47^{phox} are present in diverse intracellular compartments of a single labeled soma (p47-s). Gold-silver deposits can be seen near rough endoplasmic reticula (rER) just beneath the nucleus (n), as well as nearby small vesicular organelles (vo). (B). A single immunogold labeled dendritic profile (p47-d) contains gold labeling for p47^{phox} (small closed arrow) near vesicular organelles (vo) and the cytoplasm. This dendritic profile is present in proximity to the neurovasculature as indicated by a vessel lumen (lu) and an associated endothelial cell (edth). (C). A single gold labeled small dendritic profile (p47-d) is present within the neuropil. This dendritic profile contains immunogold labeling on the extrasynaptic surface membrane adjacent to an unlabeled axon terminal (ut) that forms an excitatory-type asymmetric synapse (closed curved arrow). Unlabeled dendritic (ud) and axon terminal (ut) profiles are seen in the nearby neuropil. (D). A small single immunoperoxidase labeled dendritic profile (p47-d) is

present within the neuropil containing unlabeled axon terminals (ut1 and ut-2). Immunoperoxidase reaction product is seen near the plasmalemma beneath an asymmetric synapse (closed curved arrow) formed by an unlabeled axon terminal (ut-1). Scale Bars = 0.5 μm.

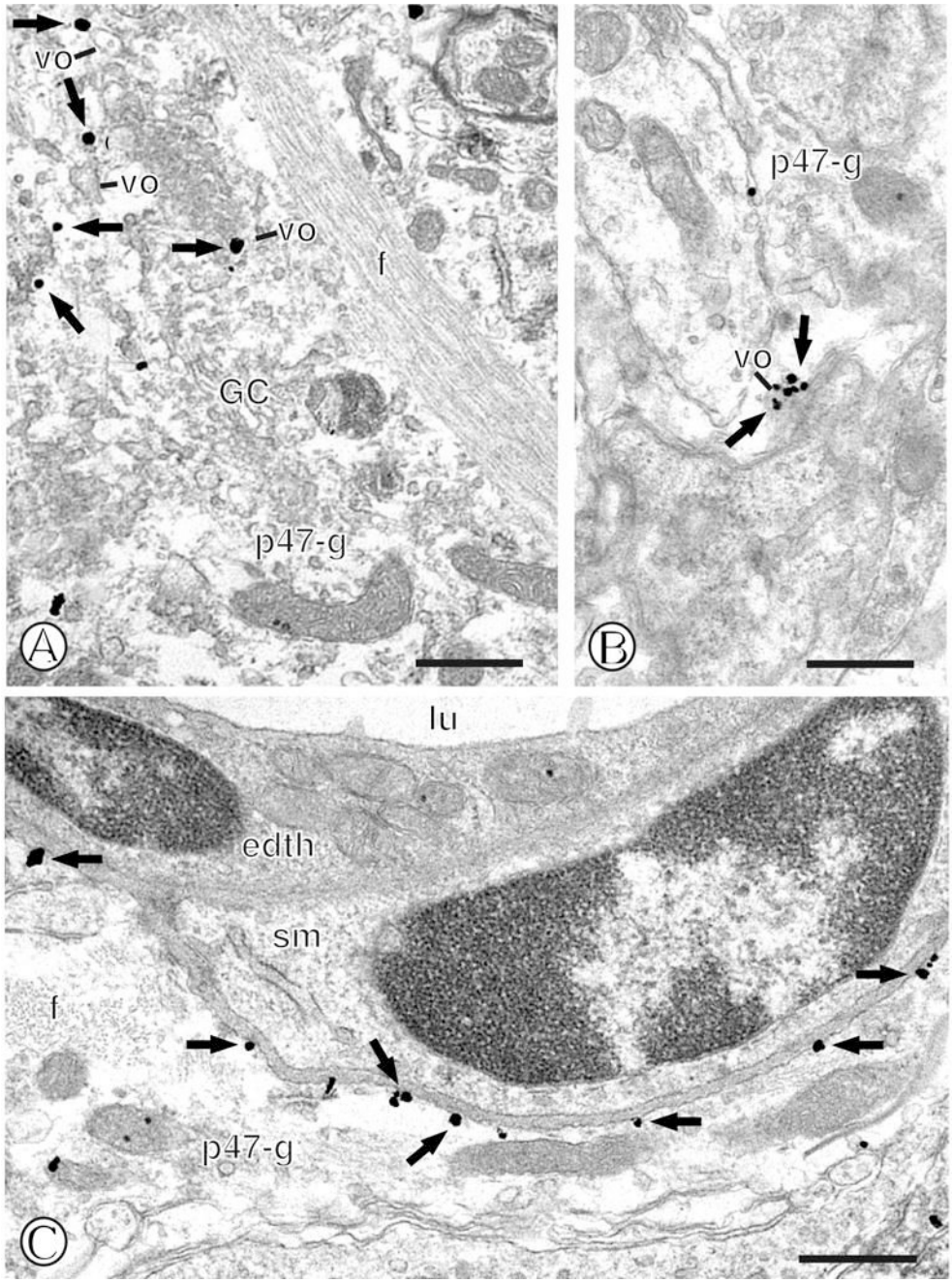

Figure 3.

Immunogold labeling of p47^{phox} in mNTS astroglia. (A). A large single labeled fibrous astroglial profile (p47-g) contains immunogold particles (small closed arrows) associated with small vesicular organelles (vo). This glial process contains extensive fiber bundles (f), a Golgi complex (GC), and numerous vesicular organelles (vo). (B). A single labeled glial process (p47-g) contains a cluster of gold particles (small closed arrows) near a dense vesicular organelle (vo). (C). A single labeled astrocytic process (p47-g) contains plasmalemmal immunogold labeling (small closed arrows). This profile, which contains a bundle of cross-sectional fibers (f), is present near a blood vessel lumen (lu) and its associated endothelial cell (edth) and a smooth muscle cell (sm). Scale Bars= 0.5 μm.

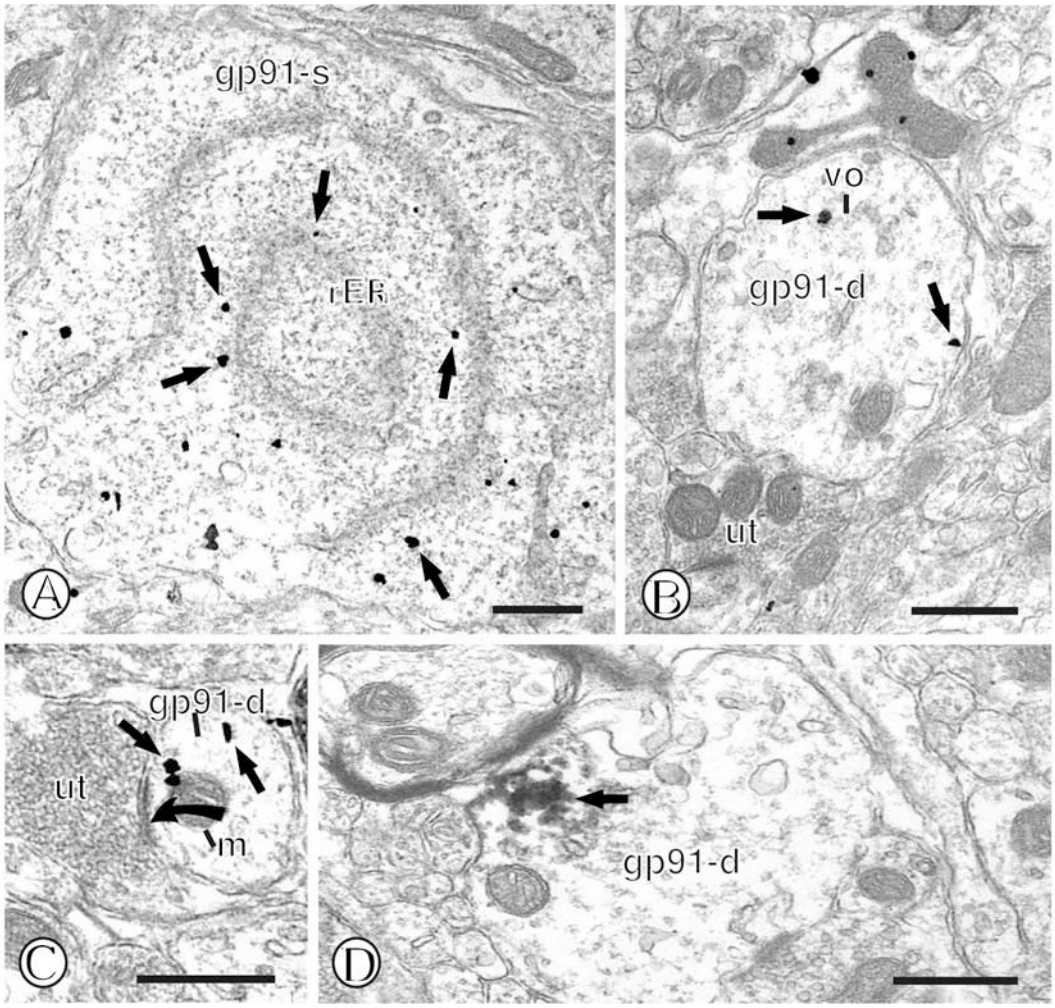

Figure 4.

Immunogold labeling of gp91^{phox} in mNTS neurons. (A). A single labeled neuronal cell body (gp91-s) contains gold particles (small closed arrows) near rough endoplasmic reticula (rER). (B). A single labeled dendritic profile (gp91-d) contains gold particles (small closed arrows) intracellularly, as well as near the extrasynaptic plasma membrane. The dendrite is apposed to an unlabeled axon terminal (ut). (C). A small dendritic profile (gp91-d) contains gold particles (small closed arrow) in diverse intracellular sites, including the cytoplasm and near a mitochondrion (m). This dendritic profile receives an asymmetric synapse (closed curved arrow) from an unlabeled axon terminal (ut). (D). A single labeled dendritic profile (gp91-d) contains a dense intracellular aggregate of immunoperoxidase reaction product (small closed arrow). Scale Bars = 0.5 μm.

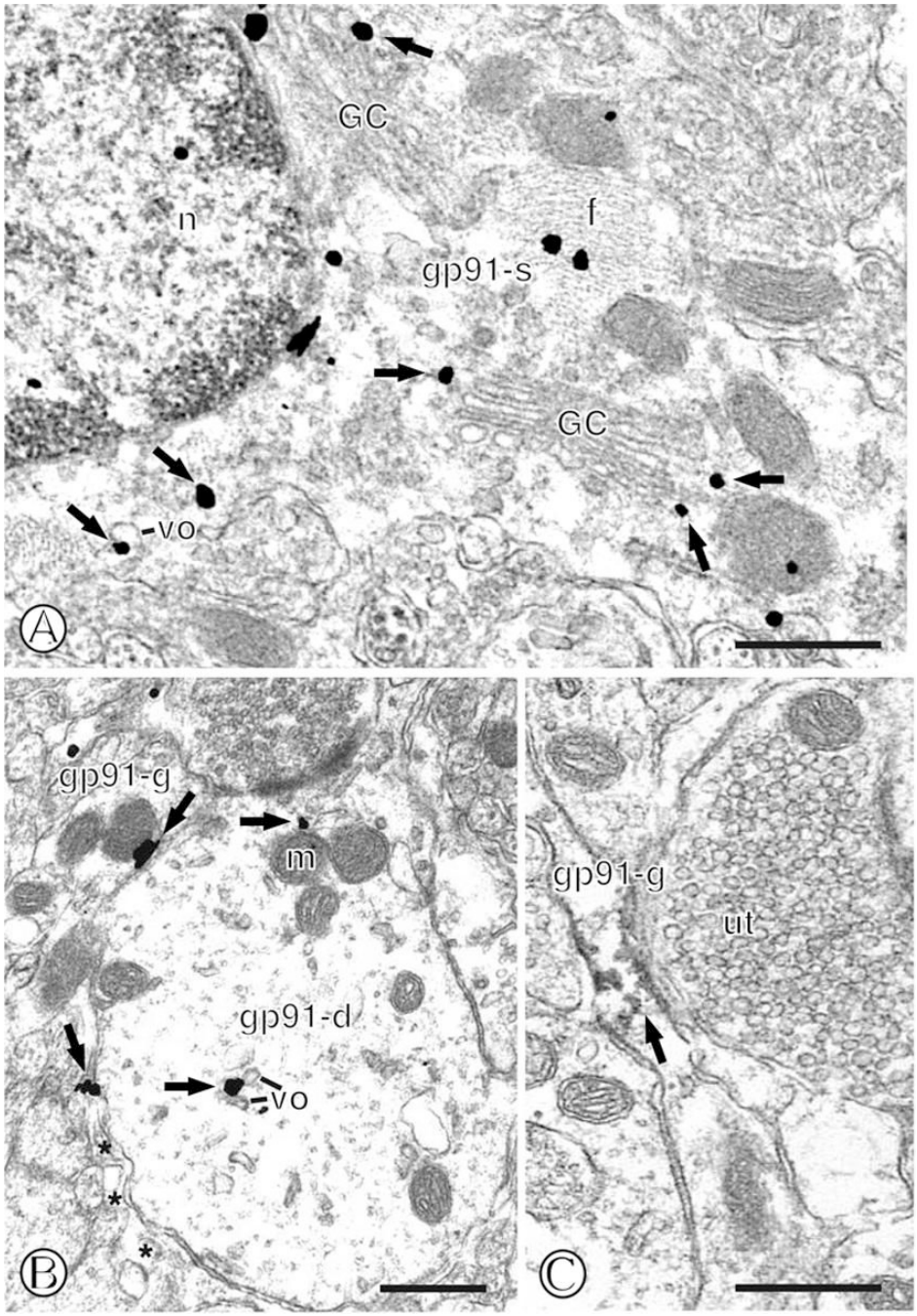

Figure 5.

Immunogold labeling of gp91^{phox} in mNTS astroglia. (A). The cell body of an astrocyte (gp91-s) containing numerous cross-sectioned fibers (f) displays immunogold particles (small closed arrows) near diverse intracellular organelles. These include Golgi complex's (GC) and vesicular organelles (vo) that surround the nucleus (n). (B). A single labeled glial process (gp91-g) contains immunogold particles (small closed arrows) near the surface membrane. This glia is apposed to a single labeled dendritic profile (gp91-d) that displays gold labeling near small vesicular organelles (vo) and a mitochondrion (m) located just beneath the postsynaptic density. (C). A small elongated glial process (gp91-g) shows immunoperoxidase

labeling (small closed arrow) intracellularly and near the surface membrane. The surrounding neuropil contains unlabeled profiles, including an axon terminal (ut). Scale Bars = 0.5 μm.

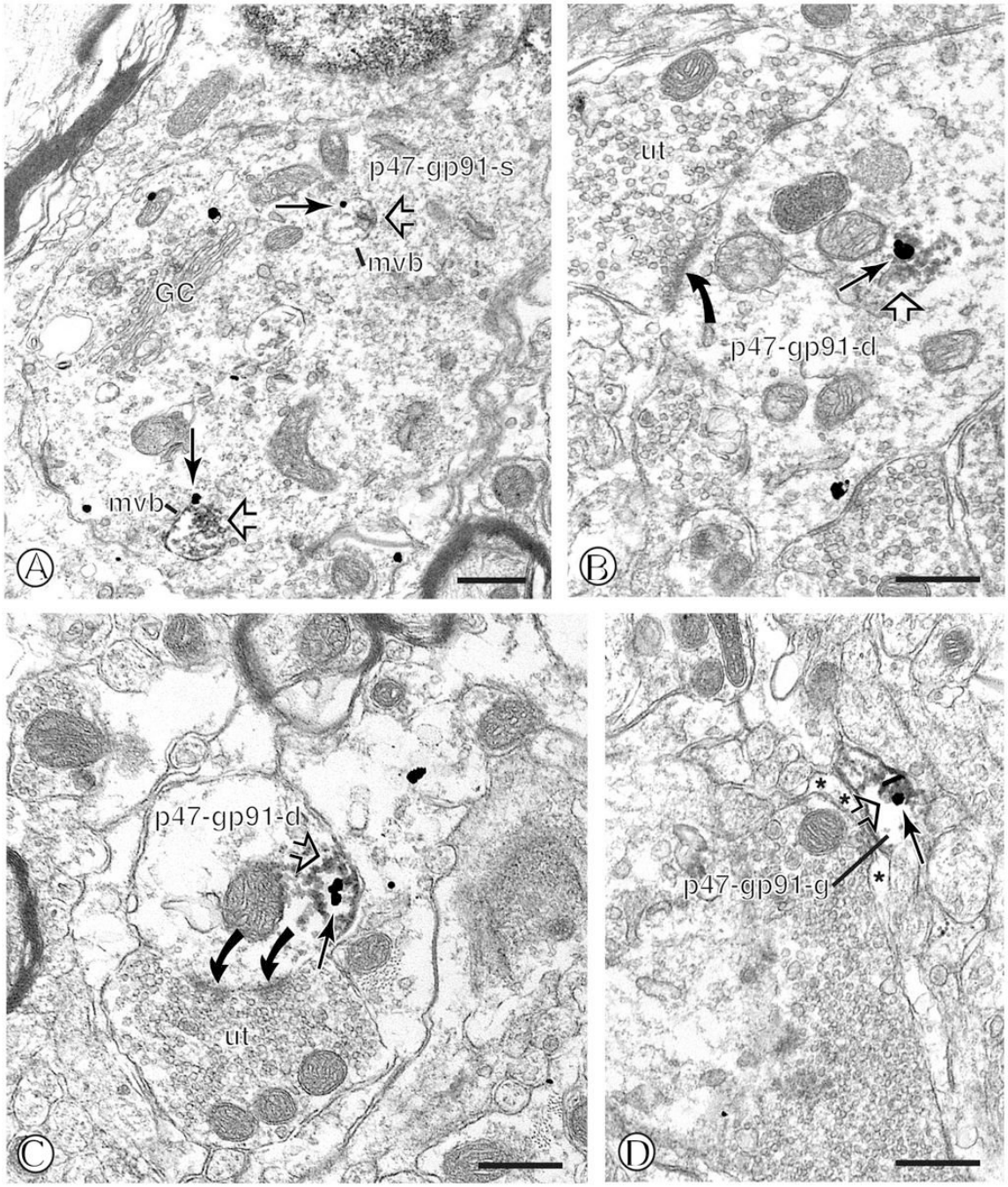

Figure 6.

Dual immunogold labeling of p47^{phox} and immunoperoxidase labeling of gp91^{phox} in mNTS neurons and astroglia. (A). A dual labeled neuronal soma (p47-gp91-s) contains large vesicular organelles characteristic of multiple vesicular bodies (mvb). These organelles contain immunogold labeling for p47^{phox} (large arrow) and aggregates of peroxidase reaction product for gp91^{phox} (open arrow) in the inner lumen. (B). A large dendritic profile (p47-gp91-d) contains overlapping intracellular immunogold p47^{phox} (large arrow) labeling and gp91^{phox} immunoperoxidase reaction product (open arrow). This dendrite is contacted by multiple axon terminals, one of which forms an asymmetric synapse (closed curved arrow) (C). A small dendritic profile (p47-gp91-d) contains overlapping p47^{phox} (large arrow) gold and gp91^{phox}

immunoperoxidase labeling (open arrow) just beneath the surface membrane. This dendritic profile is contacted by an unlabeled axon terminal (ut) forming a perforated asymmetric synapse (curved closed arrows). (D). A small glial process (p47-gp91-g) shows overlapping $p47^{phox}$ immunogold (large arrow) and $gp91^{phox}$ immunoperoxidase labeling (open arrow) near the surface membrane. Asterisks= unlabeled glia. found Scale Bars = 0.5 μm.

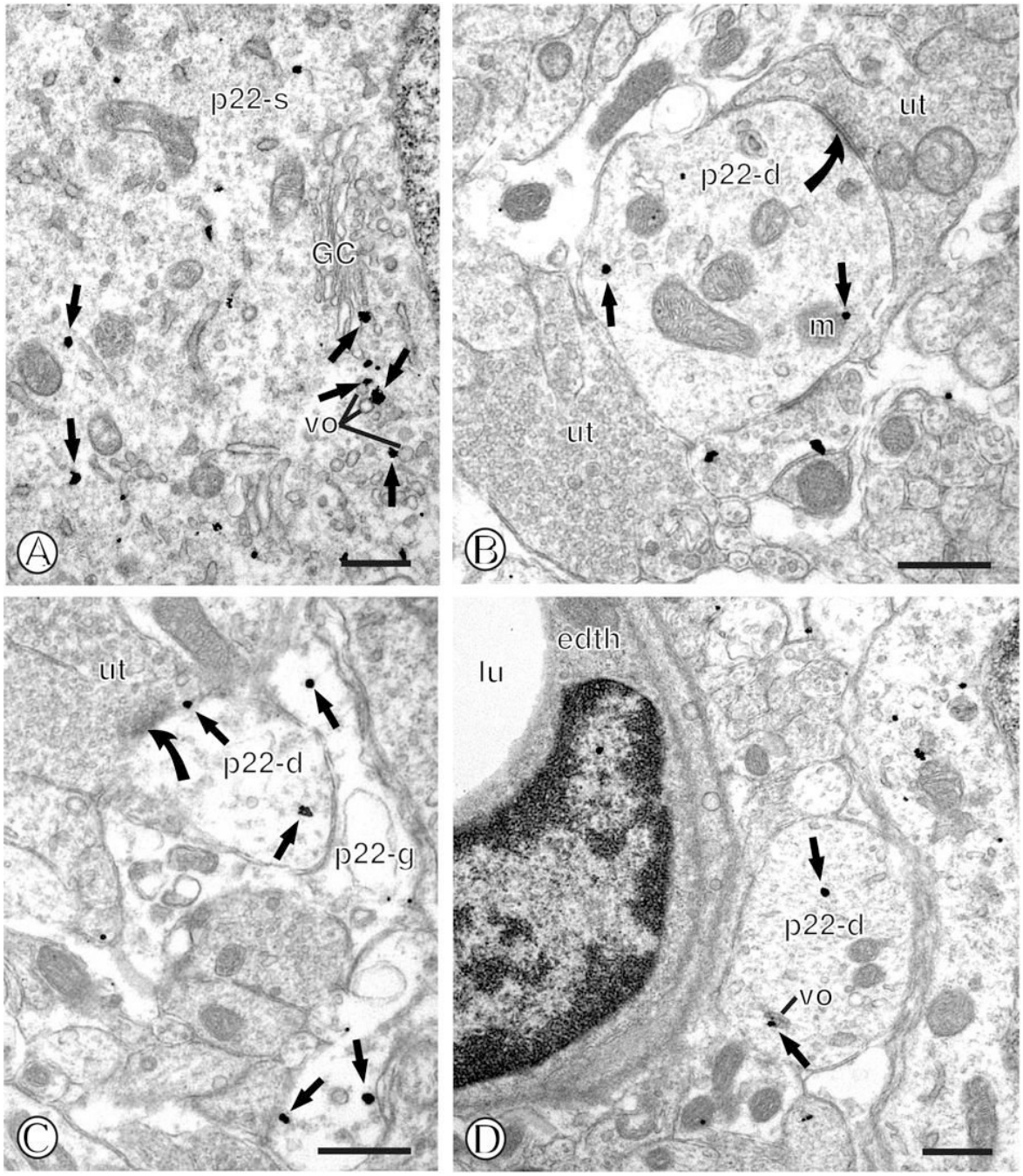

Figure 7.

Immunolabeling of p22^{phox} in mNTS neurons. (A). A neuronal cell body (p22-s) contains immunogold labeling (small closed arrows) in association with diverse intracellular organelles, including a Golgi complex (GC), and small round vesicles (vo). (B). A dendritic profile (p22-d) contains an intracellular gold particle (small closed arrow) near a mitochondrion (m). This profile is contacted by unlabeled axon terminals (ut), one of which forms an asymmetric synapse (closed curved arrow). (C). A small dendritic profile (p22-d) contains gold particle at diverse sites, including the perisynaptic plasmalemma (small closed arrow) near the postsynaptic density of an asymmetric synapse (closed curved arrow) formed by an unlabeled axon terminal (ut). This dendritic profile is also contacted by an immunogold labeled glial

process (p22-g). (D). A single labeled dendritic profile (p22-d) contains an intracellular gold particle (small closed arrow) near a small vesicular organelle (vo). This dendritic process is located near a blood vessel, as seen by the vessel lumen (lu) and associated endothelial cell (edth). Scale Bars = 0.5 μm.

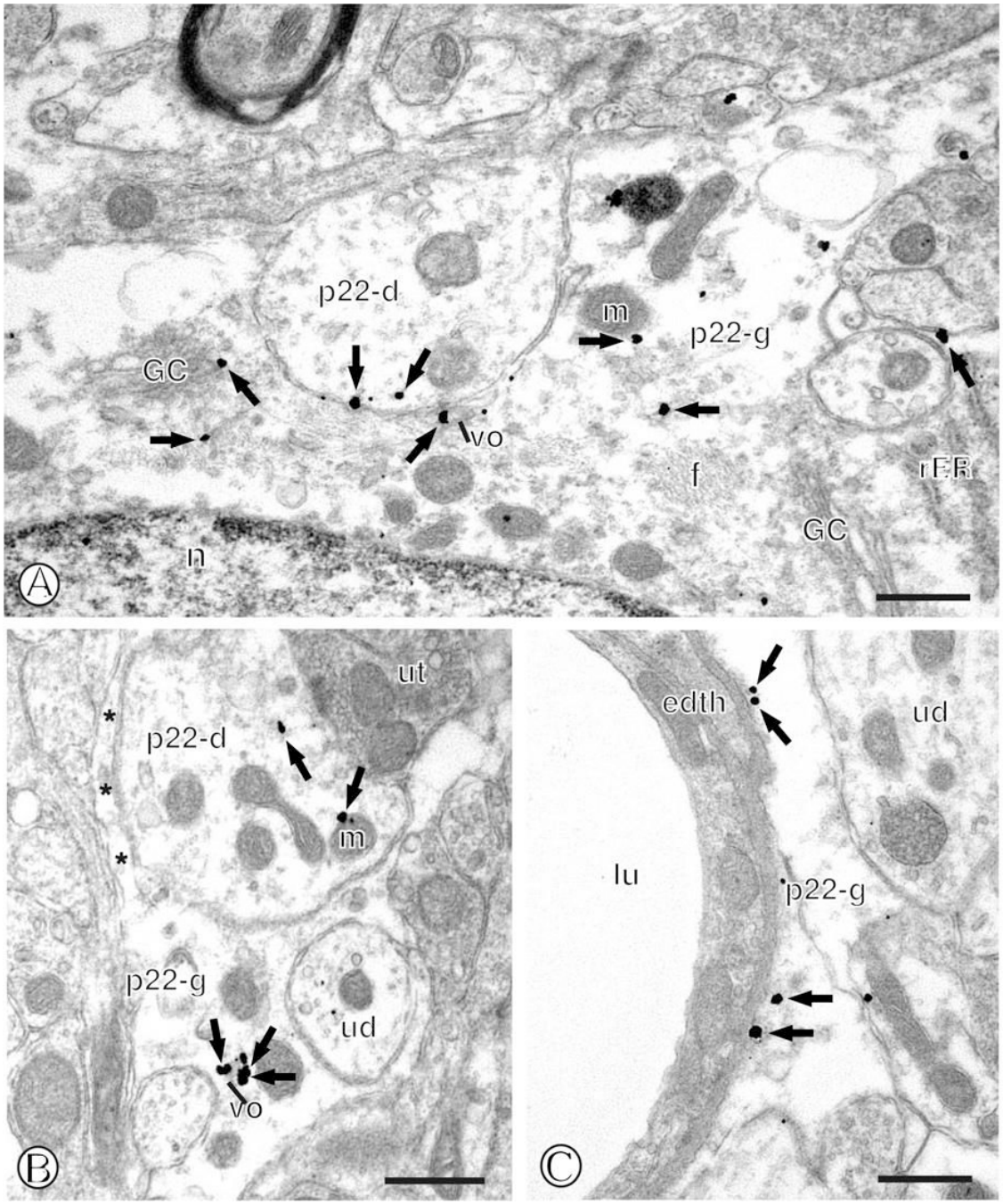

Figure 8.

Immunolabeling of p22^{phox} in mNTS astroglia. (A). The cell body of an astroglia (p22-g) contains gold particles (small closed arrows) in association with a Golgi complex (GC), vesicular organelles (vo) and the surface membrane. A dendritic profile (p22-d) apposes this glial profile. (B). A glial process (p22-g) contains an aggregation of gold particles (small closed arrows) near a vesicular organelle (vo). A single labeled dendritic profile (p22-d) is directly apposed to this glial process. (C). A single labeled glial process (p22-g) contains gold particles near the surface membrane just beneath the basal lamina surrounding an endothelial cell (edth) and vessel lumen (lu). Asterisks= unlabeled glia. Scale Bars = 0.5 μm.

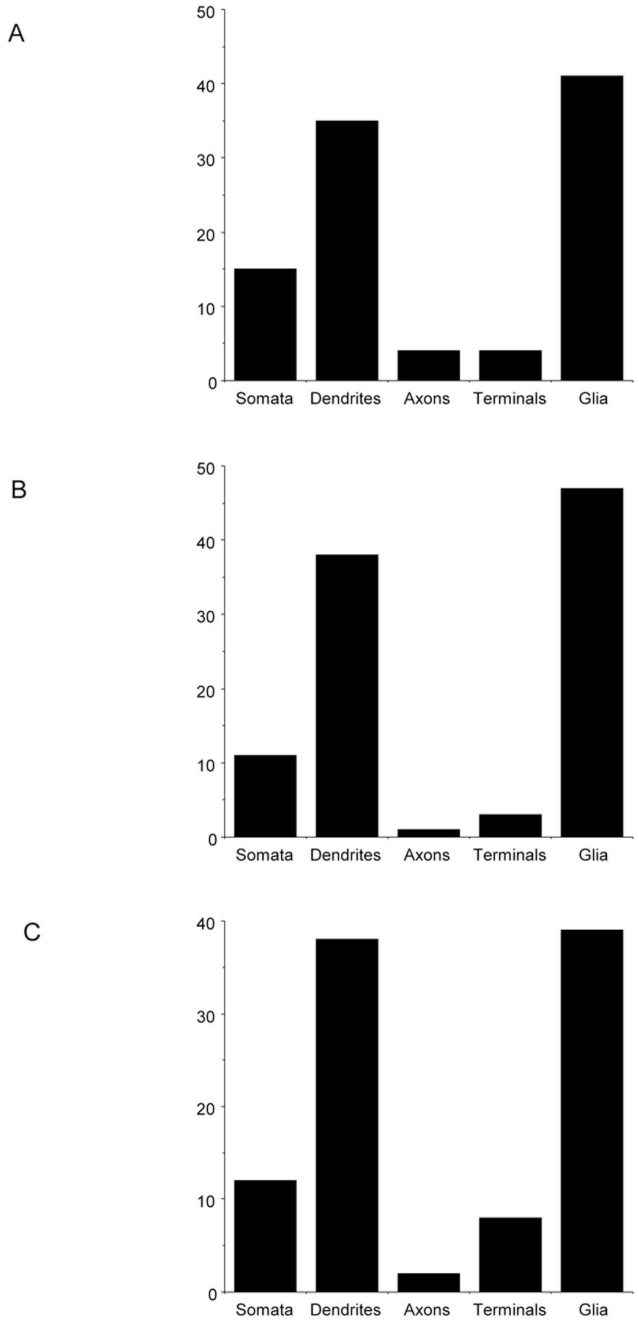

Figure 9.

Quantification of NADPH oxidase subunits in mNTS neuronal and astroglial profiles. (A). There is a differential distribution of $p47^{phox}$ immunogold labeling in neuronal compartments and in astroglia in the mNTS. In neuronal profiles, labeling of $p47^{phox}$ was most prominent in somata and dendrites. There was also substantial labeling within glial processes. (B and C). Similar to $p47^{phox}$, labeling of $gp91^{phox}$ and $p22^{phox}$ in the mNTS is mainly present in somatodendritic profiles, as well as astroglia.

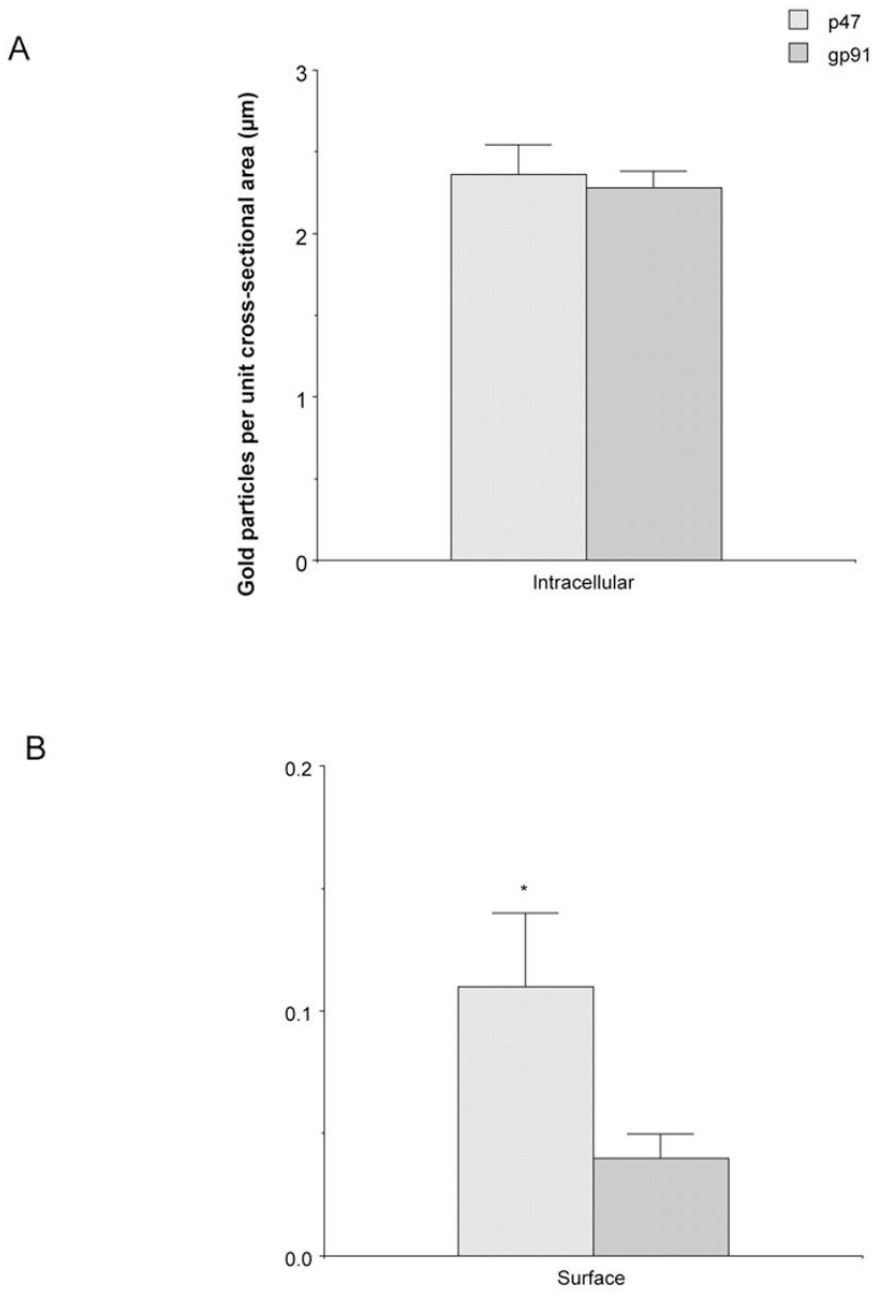

Figure 10.

Quantification of the subcellular localization of NADPH oxidase subunits in mNTS neuronal profiles. (A). The number of $p47^{phox}$ and $gp91^{phox}$ immunogold particles per unit cross-sectional area is similar in mNTS neurons. (B). There is a higher density of $p47^{phox}$ gold particles per unit surface area relative to $gp91^{phox}$ gold labeling in mNTS neurons. Data presented as mean±SEM. *=$p<0.05$.

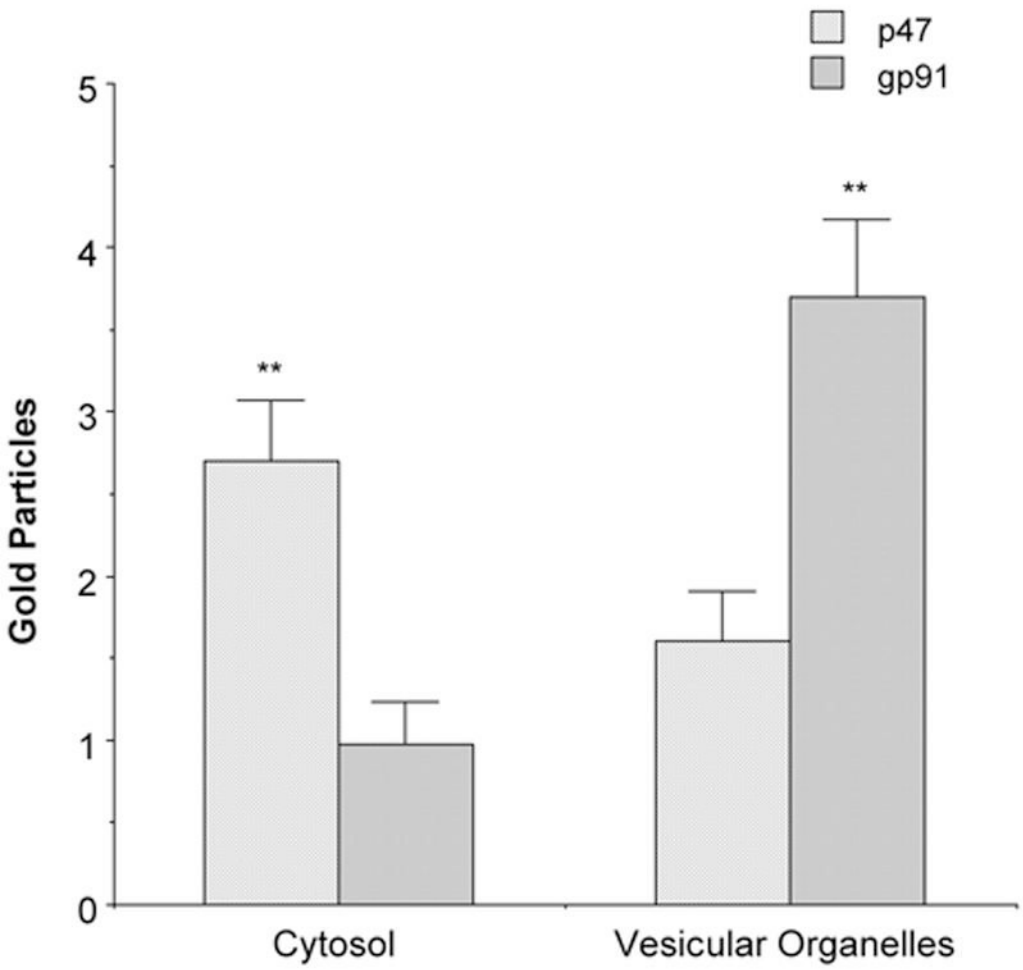

Figure 11.

Quantification of the subcellular localization of NADPH oxidase subunits in mNTS astroglial profiles. Immunogold labeling of NADPH oxidase subunits are differentially distributed in intracellular compartments in mNTS glia. There is a higher level of $p47^{phox}$ labeling associated with the cytosol compared to $gp91^{phox}$. In contrast, $gp91^{phox}$ is more prevalent in association with vesicular organelles. **=$p<0.01$.

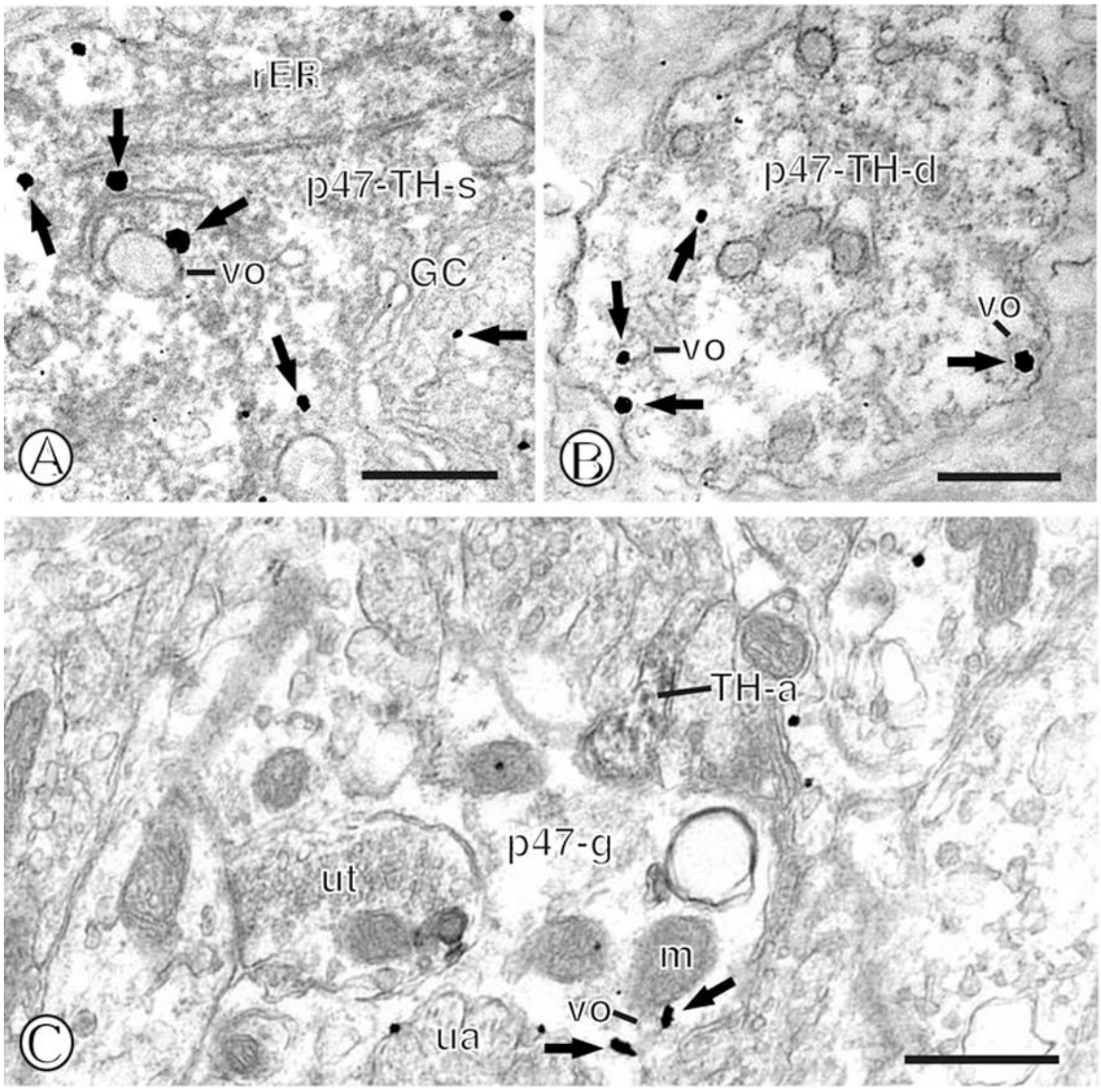

Figure 12.

Dual immunolabeling of p47^{phox} and TH in mNTS neurons or astroglia. (A). A dual labeled soma (p47-TH-s) containing diffuse immunoperoxidase reaction product for TH also shows immunogold p47^{phox} labeling (small closed arrows) in association with diverse intracellular organelles, including rough endoplasmic reticula (rER) and a Golgi complex (GC). (B). A dual labeled dendritic profile (p47-TH-d) shows dispersed immunoperoxidase immunoreactivity for TH and immunogold labeling of p47^{phox} (small closed arrows) near vesicular organelles (vo) and the plasma membrane. (C). A single labeled glial process (p47-g) contains immunogold-silver deposits (small closed arrows) near a mitochondrion (m) a vesicular organelle (vo) and the surface membrane. This glial profile is contacted by a small axon (TH-a) containing TH immunoperoxidase labeling. Scale Bars = 0.5 μm.

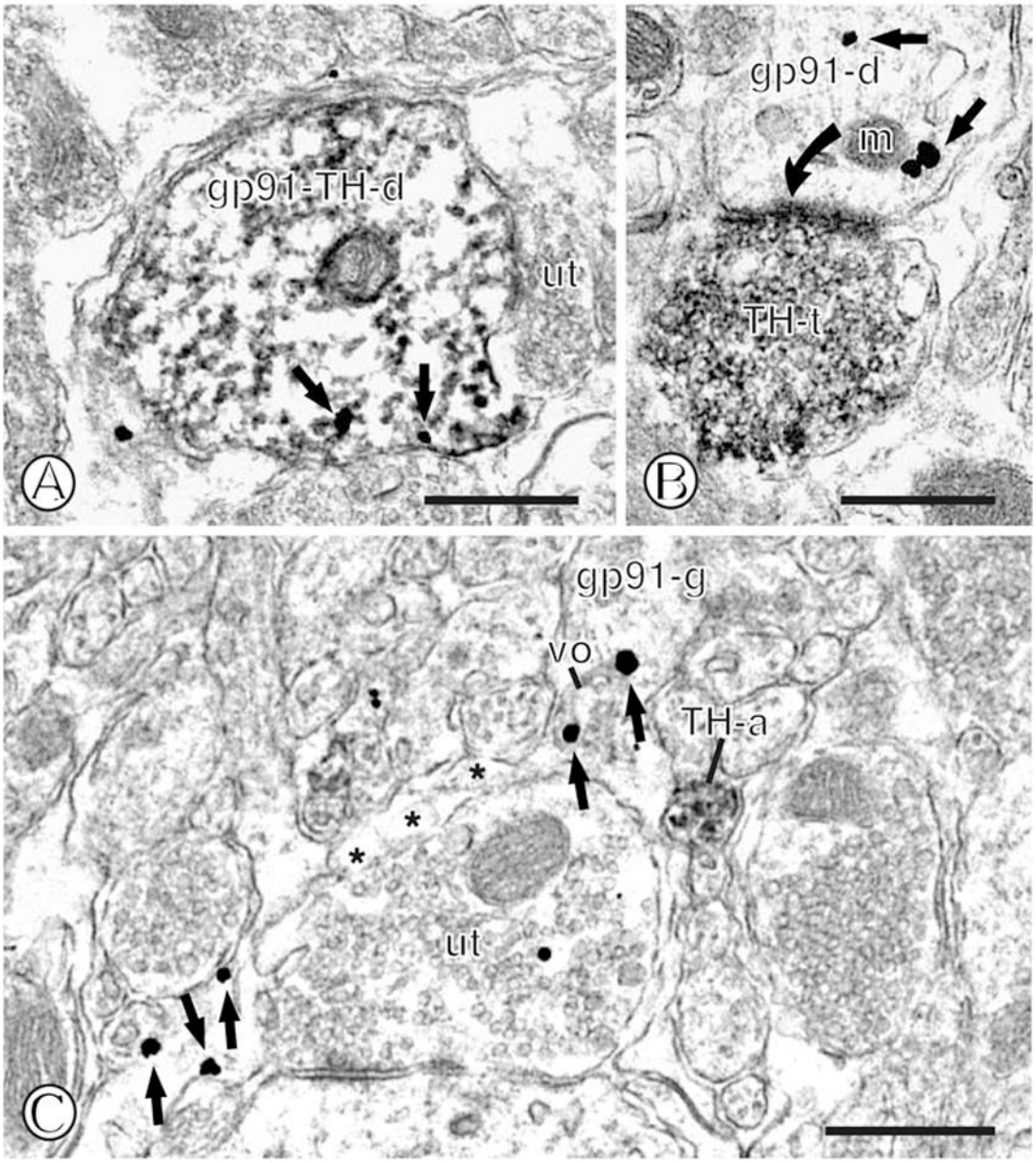

Figure 13.

Dual immunolabeling of gp91^{phox} and TH in mNTS neurons or astroglia. (A). A dual labeled dendritic profile (gp91-TH-d) displays diffuse immunoperoxidase reaction product for TH. Immunogold particles (small closed arrows) are present intracellularly and near the surface membrane adjacent to an unlabeled axon terminal (ut). (B). A single gp91^{phox} labeled dendritic profile (gp91-d) contains intracellular immunogold labeling (small closed arrows), including near a mitochondria (m). This dendrite receives an asymmetric type synapse (curved closed arrow) from an axon terminal (TH-t) showing dense immunoperoxidase reaction product for TH. (C). A single labeled glial process (gp91-g) contains dispersed immunogold particles (small closed arrows) near a vesicular organelle (vo) and the plasmalemma. This glia is contacted by numerous neuronal profiles, including an unlabeled axon terminal (ut) and a small immunoperoxidase labeled unmyelinated axon (TH-a). Scale Bars = 0.5 μm.

TABLE 1A

Subcellular distribution of phox immunogold labeling in mNTS dendritic profiles

	Surface	Intracellular	vesicular	mitochondrial	cytosolic
$p47^{phox}$	0.5±.1*	2.2±.2	1.5±.1	0.2±.1	0.6±.1
$gp91^{phox}$	0.2±.1	2.3±.2	1.3±.2	0.3±.1	0.6±.2

TABLE 1B

Subcellular distribution of phox immunogold labeling in mNTS glial profiles

	Surface	Intracellular vesicular	mitochondrial	cytosolic
$p47^{phox}$	0.8±.3	4.2±.4	3.0±.3	19±.1	1.0±.2
$gp91^{phox}$	1.0±.2	5.5±.7	4.5±.6*	0.4±.1	0.6±.2